Optofluidics incorporating actively controlled micro- and nano-particles

Aminuddin A. Kayani,[1,a)] Khashayar Khoshmanesh,[1,2] Stephanie A. Ward,[3] Arnan Mitchell,[1] and Kourosh Kalantar-zadeh[1,a)]
[1]*School of Electrical and Computer Engineering, RMIT University, Melbourne, Victoria 3001, Australia*
[2]*Department of Mechanical Engineering, Stanford University, Stanford, California 94305, USA*
[3]*Monash Ageing Research Centre (MONARC), Monash University, The Kingston Centre, Victoria 3192, Australia*

(Received 23 April 2012; accepted 25 June 2012; published online 18 July 2012)

The advent of optofluidic systems incorporating suspended particles has resulted in the emergence of novel applications. Such systems operate based on the fact that suspended particles can be manipulated using well-appointed active forces, and their motions, locations and local concentrations can be controlled. These forces can be exerted on both individual and clusters of particles. Having the capability to manipulate suspended particles gives users the ability for tuning the physical and, to some extent, the chemical properties of the suspension media, which addresses the needs of various advanced optofluidic systems. Additionally, the incorporation of particles results in the realization of novel optofluidic solutions used for creating optical components and sensing platforms. In this review, we present different types of active forces that are used for particle manipulations and the resulting optofluidic systems incorporating them. These systems include optical components, optofluidic detection and analysis platforms, plasmonics and Raman systems, thermal and energy related systems, and platforms specifically incorporating biological particles. We conclude the review with a discussion of future perspectives, which are expected to further advance this rapidly growing field. [http://dx.doi.org/10.1063/1.4736796]

I. INTRODUCTION

Optofluidics refers to the field of research involving the integration of microfluidics and optics in the same platform, where fluid and light are driven to interact.[1] This integration has led to the realization of a wide range of applications such as optical sources,[2] lenses,[3] beam manipulators,[4] particle transport,[5] and sensing[6] in liquid media. Optofluidics is also used to describe a class of optical systems that are synthesized with fluids. Fluids have unique properties that cannot be found in solid equivalents, and hence these properties have been used for designing novel devices. Examples of such properties include the ability to change the optical property of the fluid medium within a device by simply replacing one fluid with another, the optically smooth interface between two immiscible fluids, and the ability of flowing streams of miscible fluids to create gradients in optical properties by diffusion.[7]

A well-established category of optofluidic devices consist of homogenous liquids with varying refractive indices.[8] However, a disadvantage of using such homogeneous liquids is that they have properties that are inflexible. In particular, obtaining a tunable and reconfigurable liquid media can be an extremely arduous task as it can only be achieved by substituting one type of liquid with another, mixing different liquids together or modifying their properties *via* chemical

[a)]Authors to whom correspondence should be addressed. Electronic addresses: akayani1@ieee.org and kourosh.kalantar@rmit.edu.au.

processes. In response to this, the incorporation of suspended particles provides functionalities capable of addressing such issues with relative ease and efficiency. However, the challenge associated with the implementation of particles is the ability to control their motion and locations such as placing them precisely where they are needed and when desired. Therefore, in realizing robust optofluidic systems incorporating particles, the pressing need is access to particle manipulation mechanisms that are able to prescribe particle movement and placements accurately.

Precise mechanisms or forces that can control the motion of suspended particles would make it possible to alter and adjust the concentration and packing of particles in the bulk of microfluidics on demand. Particles could then be scattered when these mechanisms and forces are removed.[9] Alternatively, particles could be sorted and lined up individually according to their intrinsic properties as a preparative process before undergoing an optical interrogation process in small dimensions.

In the past five years, several important reviews on the matter of particles and optofluidics were reported. Despite these reviews, we have found that the subject matter of our review has not been specifically covered in literature. The review by Lee *et al.*,[10] for example, focuses primarily on surface enhance Raman spectroscopy (SERS) and plasmonic applications of colloidal optofluidics. In addition, the reviews by Tsutsui and Ho[11] and Lenshof and Laurell[12] describe particle and cell separations in microfluidic systems but do not concentrate on optofluidic devices and systems. The review on tuneable optofluidics by Levy and Shamai[13] covers indiscriminately examples of optofluidic systems integrated with suspended particles; however, it does not constitute the bulk of the review. Our observation is that these reviews did not cover the fundamentals of particle manipulation and their applications in optofluidics, which would be extremely useful, especially for researchers needing a fundamental reference and those exploring this field for the first time.

In this review, we aim to address this niche research field. We begin by presenting different types of particle manipulation forces in microfluidic systems with a focus that is confined to "actively applied" forces, which are capable of generating accurate and consistent particle motions. Our intent is not to present an in depth analysis but rather to canvas the fundamentals, which have some bearing on understanding and applying these forces effectively. Subsequently, we present the most pertinent and novel optofluidic applications, which have resulted from the incorporation of such well controlled suspended particles.

II. MANIPULATION OF SUSPENDED MICRO- AND NANO-PARTICLES

Particles can be manipulated either "passively" or "actively." Passive manipulation forces include Van der Waals attraction,[14] self assembly,[15] stearic interaction,[16] Brownian motion,[17] and charged dipole interaction.[18] Unfortunately, such passive manipulation techniques[19–22] are not capable of high levels of control, consistency, and repeatability.[11]

In contrast, active forces are externally applied and are able to provide particle displacements and motional trajectories, which are consistent and precise to a high degree of accuracy. The opportunities for realizing optofluidic systems incorporating such precise particle motions are therefore much more promising. In this review, we will focus on elaborating such active forces and particle manipulation techniques, which can be achieved using them. We classify these active forces into mechanical,[23–27] electrical,[28–32] optical,[33,34] thermal,[35–37] and magnetic[38–40] force categories.

A. Mechanical

Particles can be manipulated in microfluidic systems using mechanically induced forces. These forces are categorized into two types, which include "hydrodynamic forces" induced motion and those forces induced by varying pressure profiles, commonly known as "acoustic forces."

1. Hydrodynamic

Hydrodynamic manipulation in microfluidic systems refers to the control of particle displacement as a result of liquid motion. These forces, which are used to manipulate the

movements of particles, are known as hydrodynamic forces. They are imposed on particles using liquid motion against them or around them, such that liquid motion is able to control particle displacements and their trajectories.[23]

Two types of liquid flows which are important in the definition of liquid motion include "Laminar flow," in which the flow experiences a smooth motion with no dispersion between the neighbouring layers, and "non-laminar flow" (also called "turbulent flow"), in which the flow experiences irregular fluctuations and eddies and cannot maintain its smooth motion.[24] Laminar and non-laminar flow behaviors are important characteristics of multi-phase liquid media as they govern the motion of suspended particles in microfluidics.

The Reynolds number, Re_d, describes the presence of Laminar or non-laminar flows. This number represents the ratio of the inertial force to the viscous force and is expressed as[25,26]

$$\mathrm{Re}_d = \frac{\rho_m v_f L}{\mu_m}, \tag{1}$$

where ρ_m is the fluid medium density, v_f is average velocity of the medium inside the microchannel, L is the equivalent diameter of the microchannel, and μ_m is the dynamic viscosity of the fluid. For the flow inside microchannels, an Re_d of less than 1000, corresponds to the Laminar regime, while an Re_d of more than 1000 corresponds to the turbulent regime.[23]

The drag force, F_{drag}, refers to the force propelling a particle as it moves through a body of fluid (Fig. 1(a)). It is proportional to the particle size, dynamic viscosity of the fluid, and the difference in fluid and particle velocities. The drag force, F_{drag}, is estimated using the Stokes law as[41]

$$F_{drag} = 6\pi\mu_m r\bar{U}, \tag{2}$$

where r is the particle radius and $\bar{U}$ is the relative velocity of the particle to the medium inside the microchannel.

One of the most common applications of hydrodynamic manipulation is the flow focusing of particles. Sheath flow focusing is one of the most commonly used methods for manipulating

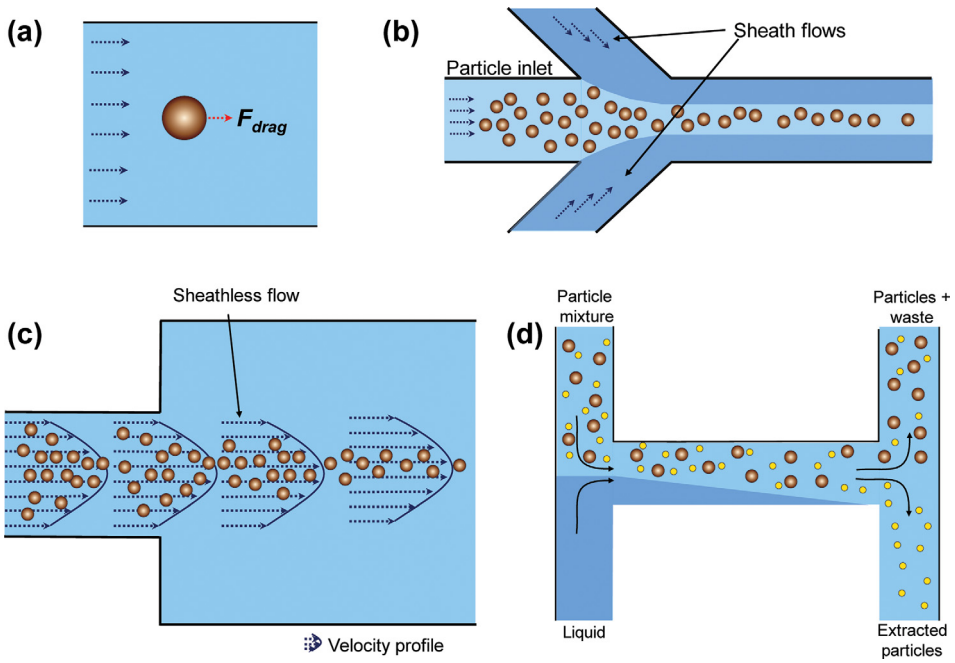

FIG. 1. Hydrodynamic particle manipulation. (a) Drag force acting on a particle under microfluidic flow; (b) sheath flow focusing; (c) sheathless flow focusing; (d) H-shaped inlet and outlet microfluidic separation system.

the position of particles by using one or more sheath fluids to pinch the particle suspension flow and thus focuses the suspended particles. In general, one or more sheath fluids should be used in order to obtain a two dimensional (2D) or three dimensional (3D) particle focusing. Figure 1(b) depicts a classic example of sheath flow focusing relying on a pair of liquid flows that sandwich a stream of liquid containing the particles.[42] This method is used in the sorting, counting, separation, and detection of particles as it provides reasonably accurate and reproducible particle trajectories in liquid.

Sheathless particle focusing is another method of manipulating particles.[42] This process does not rely on a pair of sheath liquid flows to focus the particles. Instead, it employs hydrodynamic drag force that induces the particles to flow to their equilibrium positions according to the velocity profile of the liquid stream (Fig. 1(c)).[43]

Hydrodynamic forces are used for particle sorting and separation applications as well.[44,45] Fig. 1(d) presents a H-shaped inlet and outlet microfluidic system that separates a solution containing a mixture of particles.[46,47] The particle mixture is a dilute solution of different-sized particles, entering from one of the inlets. A particle-free flow enters from the other inlet. The separation is based on the non-mixing nature of two adjacent flows at low Reynolds numbers in conjunction with the fast diffusion of small particles compared to bigger ones. The length of the mixing channel was carefully chosen so that small particles could diffuse across the channel before reaching the output channel.

Hydrodynamic traps in the form of microfluidic stagnation points, micro-vortices, or micro-eddies can also manipulate the motion of particles in liquid.[48,49] These traps are realized using cross-flow forces of two or more opposing laminar streams of liquid which meet at an intersection. As the opposing liquid streams meet, a flow field with a stagnation point, where the particles are trapped, is generated. This entrapment provides high resolution manipulation of a small quantity of particles. The inclusion of such methods in present day optofluidic devices is still quite rare and we will certainly see more of them used in future systems.

The motion of particles using hydrodynamic forces is affected by channel topology and uses carefully selected flow rates at which the suspended particles are able to form the desired flow trajectory or particle assembly.[44] This requires meticulous design and simulation of microfluidic flow rates, understanding of the forces affecting particles and channel geometries. However, understanding of liquid flow trajectories under various conditions provides reasonable particle control abilities.

2. Acoustic

Acoustic waves of varying pressure profiles induce an acoustic force on the particles, which causes them to move.[50,51] The process of manipulating particles using such acoustic forces is called acoustophoresis. The acoustic waves are typically generated by inter-digitated, ultrasonic, or piezoelectric acoustic transducers.[52,53]

When a suspended spherical particle is subjected to a standing wave acoustic force, the particle experiences an acoustic force, F_r, which is given by[50]

$$F_r = -\left(\frac{\pi P_o^2 V_p \beta_m}{2\lambda}\right) \cdot \phi(\beta, \rho) \cdot \sin\left(\frac{2\pi x}{\lambda}\right), \tag{3}$$

$$\varphi(\beta, \rho) = \frac{5\rho_p - 2\rho_m}{2\rho_p + \rho_m} - \frac{\beta_p}{\beta_m}, \tag{4}$$

where P_0 is the pressure amplitude of the acoustic wave, V_p is the particle volume, β and ρ are the particle or liquid compressibilities and densities, respectively, λ is the wavelength of the acoustic wave, and x is the distance to the nearest pressure node. Subscripts p and m denote particle and suspending medium, respectively. The acoustic force experienced by a particle is influenced by the magnitude and frequency of the acoustic waves, the size and elasticity of the particle, and the liquid that surrounds it.

Particles exposed to the acoustic standing wave are either pushed to the pressure nodes or the pressure anti-nodes (Fig. 2(a)). The pressure node is the location where the standing surface acoustic waves form a pressure minimum, while the pressure anti-node is the location where the acoustic waves form a pressure maximum in the liquid.[54] The direction of particle motion depends on the polarity of the φ-factor (Eq. (4)). For example, if $\varphi > 0$, particles will balance toward the pressure nodes and if $\varphi < 0$, particles will balance toward the pressure anti-nodes (Fig. 2(b)).

Acoustic manipulation of particles provides the ability to separate particles of similar sizes and densities. If one particle is more compressible than the liquid, while another is less compressible, the acoustic force displacing the two particles will be in the opposite direction, causing them to separate. As such, a mixture of particles can be trapped and sorted by the acoustic field and collected at different outlets of a microfluidic channel.[55]

Acoustic manipulation has been applied for the concentration[56] and separation[57] of particles. The drawbacks of acoustophoresis arise from the difficulty of integrating acoustic transducers into microfluidic devices, the difficulty of controlling small nano-scale particles, and the fact that particle separations can only be conducted by virtue of their size, density, and compressibility differences.[27,57]

B. Electrical

Particles can be manipulated in microfluidic systems using electrically induced forces. These forces are generally grouped into the electrophoretic and dielectrophoretic (DEP) forces. They are applied using electrically generated uniform and non-uniform electric fields, for charged and neutral particles suspended in liquid, respectively.

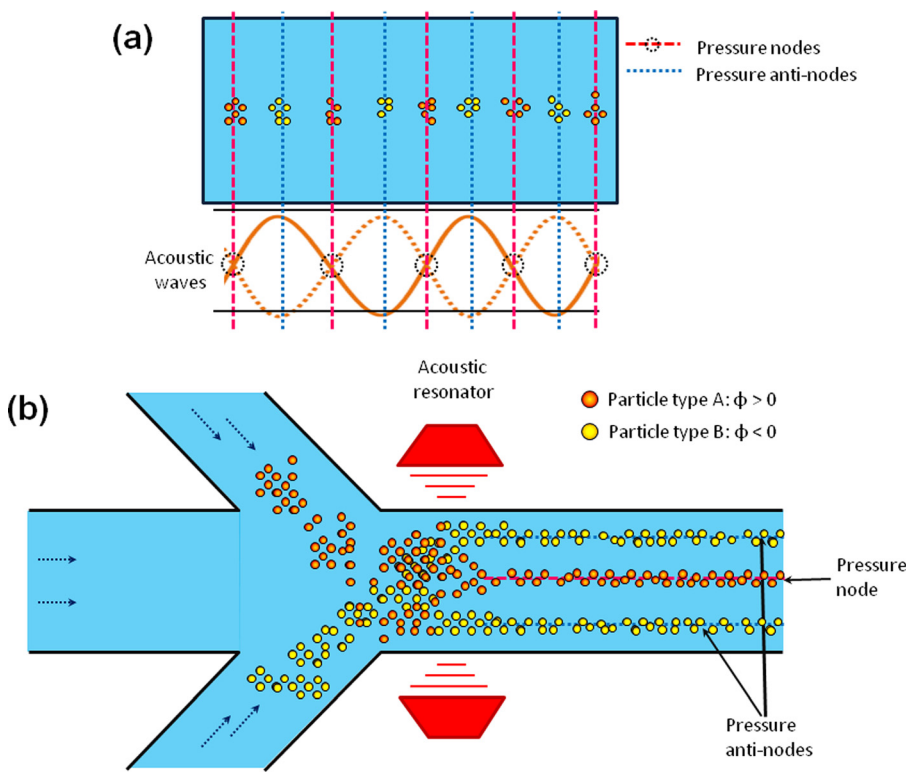

FIG. 2. Acoustophoretic manipulation of suspended particles. (a) Acoustophoretic manipulation of particles when subject to acoustic waves. (b) Schematic of acoustophoretic sorting of a mixture of particles with different density and compressibility properties.

1. Electrophoresis

"Electrophoresis" refers to the motion of charged particles, relative to a fluid, under the influence of an electric field.[32] The induced motion depends on the polarity and magnitude of the net electrical charge of the particle. Generally, electrophoretic force is generated by a pair of electrodes connected to a direct current (DC) power source. The electrodes are placed in an ionic solution which contains the particles. When the electric field is applied, particles experience an electrophoretic force, F_{el}, which induces motion toward the electrode bearing the opposite charge polarity to that of the particle (Fig. 3).[58]

There are also two forces that oppose the particles' movement: the "friction" and "electrophoretic retardation" forces. The friction force, F_{fr}, is the viscous force opposing the electrophoretically induced motion of the particle as it moves through the body of a liquid.[59] The friction force is dependant upon the viscosity of the liquid medium, as well as the size and shape of the particle. For example, larger particles moving in a more viscous liquid medium experience a higher friction force compared with smaller particles moving in a less viscous liquid medium. The electrophoretic retardation force, F_{ret}, refers to the force exerted on the diffuse cloud of ions surrounding the particle known as the "Debye layer." The ions in the Debye layer have the opposite charge polarity to the particle and therefore the electrophoretic retardation force results in a fluid flow around the particle.[60] The direction of fluid flow is in the opposing direction to the electrophoretic force. This fluid flow causes a frictional drag that is partially transferred to the particle, causing a "retardation" of the electrophoretically induced motion.

Electrophoretic mobility, μ_{el}, is a measure of charged particle mobility when subjected to an electric field. In the case of low Reynolds number and moderate electric field strength E, the electrophoretic mobility μ_{el} defined as

$$\mu_{el} = \frac{v}{E}, \tag{5}$$

where v is the velocity of the suspended particle. The electrophoretic mobility relation can be expressed as[59]

$$\mu_{el} = \frac{\varepsilon_r \varepsilon_o \varsigma}{\eta}, \tag{6}$$

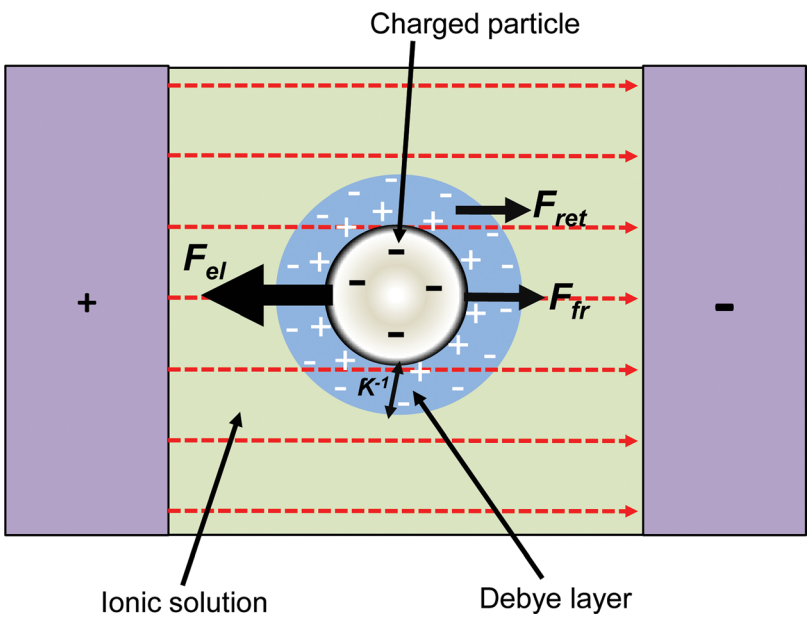

FIG. 3. Schematic of a particle experiencing the electrophoretic force.

where ε_r is the relative permittivity of the particle, ζ is the zeta potential, and η is the viscosity of the surrounding liquid. ζ is defined as[59]

$$\varsigma = \frac{\sigma r}{\varepsilon(1+\kappa r)}. \tag{7}$$

Smoluchowski's electrophoretic mobility theory is valid only for a sufficiently thin Debye length, when particle radius r is much greater than the Debye length of a charged particle such that $\kappa r \gg 1$(where κ^{-1} is the Debye length). In the case when the Debye layer is larger than the particle radius such that $\kappa r \ll 1$, Huckel established the electrophoretic mobility relation as[59]

$$\mu_{el} = \frac{2\varepsilon_r \varepsilon_o \varsigma}{3\eta}. \tag{8}$$

Electrophoretic manipulation of particles has been used in the analyses and preparative separations of biological samples, such as proteins, peptides, deoxyribonucleic acid (DNA), and ribonucleic acid (RNA) molecules.[31] It is also widely used in liquid purification processes and for the characterization of particles and their surface properties.[59]

2. Dielectrophoresis

Dielectrophoresis is the motion of neutral or semi-conducting particles induced by a spatially non-uniform electric field.[61] When subjected to a spatially non-uniform electric field, a neutral particle is polarized and charged dipoles are established within the particle. The charged dipoles induce unequal Columbic forces at opposing ends of the particles and the net resulting force causes the particles to move. The magnitude of charge and orientation of the induced dipoles is dependent on the intensity and frequency of the electric field and the dielectric properties of the particle and suspending medium, respectively.[28]

The DEP force is typically generated by a pair of closely spaced microelectrodes. They can be used as individual pairs but more often they are used as an array in a microfluidic device. The purpose of the electrodes is to transport, focus, or repel the particles from regions of interested in the microfluidics. The intensity of the applied electric field is generally highest in the regions between closely spaced electrodes. The electrodes are connected to an alternating current (AC) power source where the magnitude and frequency of the applied AC signal can be varied to achieve the desired particle motion in liquid.

For a spherical particle, the DEP force is given by[61]

$$\vec{F}_{DEP} = 2\pi r^3 \varepsilon_o \varepsilon_r \mathrm{Re}[f_{CM}(\omega)] \nabla E_{rms}^2, \tag{9}$$

where r is the radius of the particle, ε_r is the permittivity of the suspending medium, $f_{CM}(\omega)$ is the Clausius-Mossotti (CM) factor, and E_{rms} is the root mean square (*rms*) of the applied electric field. The CM factor is expressed as[28]

$$f_{CM}(\omega) = \frac{\varepsilon_p^* - \varepsilon_m^*}{\varepsilon_p^* + 2\varepsilon_m^*}. \tag{10}$$

The complex permittivity of the particle and the suspending medium, ε_p^* and ε_m^*, are given by[61]

$$\varepsilon_p^* = \varepsilon_o \varepsilon_p - i\frac{\sigma_p}{\omega}, \tag{11}$$

$$\varepsilon_m^* = \varepsilon_o \varepsilon_m - i\frac{\sigma_m}{\omega}, \tag{12}$$

where $i = \sqrt{-1}$, σ_m and σ_p are the conductivities of the medium or the particle, respectively, and ω is the angular frequency of the applied electric field.

Particles experiencing the DEP force are either attracted to or repelled from the region of high electric field gradients.[61] The sign of the Re$[f_{CM}(\omega)]$ gives an indication of the behavior of the particles in response to an applied DEP signal frequency. For instance, when Re$[f_{CM}(\omega)] > 0$, particles experience a positive DEP force such that they are attracted toward regions of high electric field gradients (Fig. 4(a)). When Re$[f_{CM}(\omega)] < 0$, particles experience a negative DEP force such that they are repelled from regions of high electric field gradients (Fig. 4(b)).[28]

Dielectrophoresis has been used in applications involving particle separation,[62] transport,[63] and sorting.[64] A drawback of DEP manipulation is the difficulty of controlling nano-scale particles, as the DEP force is proportional to r^3 and the accuracy of particle motion relies on the design of the DEP electrodes and the microfluidics. Recent reviews on DEP particle manipulation have been reported in literature.[30,65,66]

C. Thermal

Thermophoresis refers to the motion of particles suspended in liquid which is induced by a thermal gradient.[67] Although this phenomenon has been known for over 150 yr, the theory is not well established.[68] It has been suggested that particle motion results from the inhomogeneity brought in by the thermal gradients in the thin layer that constitutes the interface between the particle and the suspension.[67]

In addition to the usual Brownian motion, particles also show a systematic drift when they are placed in a thermal gradient.[69] In the presence of such a thermal gradient, the mass flux of particle flow, J, in liquid is expressed as[36]

$$J = -D\nabla c - cD_T\nabla T, \tag{13}$$

where c the particle concentration, D is the Brownian diffusion coefficient, D_T is the thermal diffusion coefficient, and ∇T is the temperature gradient. The thermal diffusion coefficient, D_T gives an indication of the particle motion behavior in a mixture in the presence of a thermal gradient. If $D_T > 0$, particles drift toward the cooler region and exhibit "thermophobic" behavior. If $D_T < 0$, particles drift towards the warmer region, exhibiting "thermophilic" behavior (Fig. 5).[36] Thermophoretic manipulation has been used for particle separation[37] and trapping.[70] Drawbacks of thermophoresis include the difficulty of transporting particles in low concentrations as they usually drift in clusters[71] and particle drift time is generally long.[72]

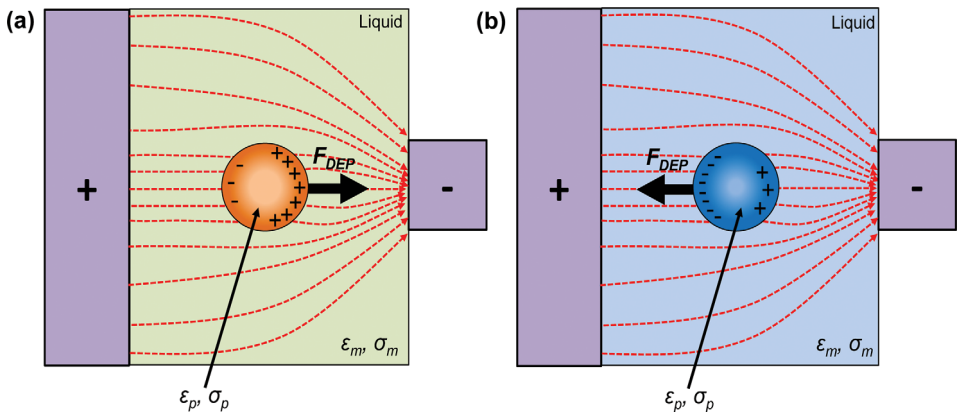

FIG. 4. Schematic of DEP manipulation of particles. (a) When Re$[f_{CM}(\omega)] > 0$, the particle experiences a positive DEP pulling it towards the region of high electric field gradients; (b) when Re$[f_{CM}(\omega)] < 0$, the particle experiences a negative DEP repelling it from the region of high electric field gradients.

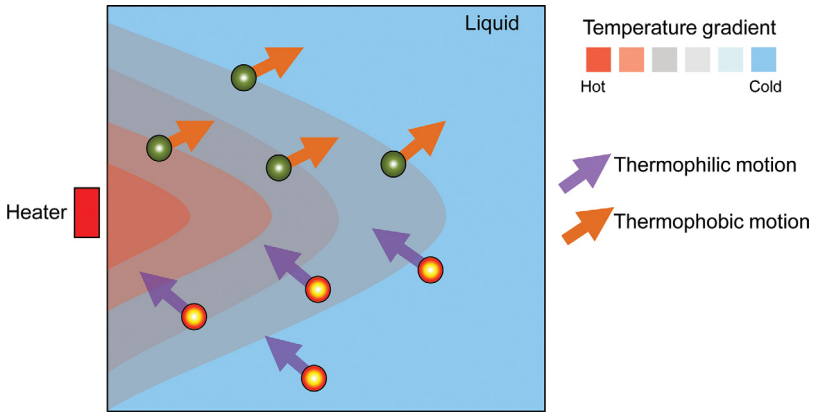

FIG. 5. Schematic of thermophoretic manipulation of particles. Thermophilic particles drift toward hotter regions, while thermophobic particles drift toward the cooler regions.

D. Optical

Optical manipulation of particles is the control of particle motion using optically induced electromagnetic fields.[73] Electromagnetic fields are generated by the radiation of light from optical sources operating in the infrared, visible, and UV range of frequencies.[34] Particles that can be manipulated using optically induced forces scale from hundreds of micrometers to a few nanometers in size[74] and are usually composed of neutral dielectrics.[75] However, the growth of near-field and plasmonic based optical manipulations (which will be described later) has expanded the type of particles that can be manipulated to include certain metallic[76,77] and semi-conducting particles.[78,79]

The interaction of particles with optical waves depends primarily on their size. Particles smaller than the wavelength of light are pulled toward the region of high electromagnetic fields as they develop an electric dipole moment in response to the light's electric field. Particles comparable or larger than the wavelength of light refract the rays of light and move as a result of a momentum transfer of the incident photons.[80] Optical manipulation of particles falls into two categories: (i) far field and near-field manipulation and (ii) plasmonic manipulation.

1. *Far and near-field manipulation*

Far field optical manipulation, commonly known as optical tweezing, refers to the control of particle motion induced by a direct irradiation of optical electromagnetic fields.[73] When a particle is subjected to this field, the optical gradient force pulls the particle toward the region of highest field intensity where the optical beam is focused.[34] Scattering and absorption forces then cause the particle to move in the direction of beam propagation (Fig. 6(a)).[33]

The optical gradient force, F_{grad}, experienced by a spherical particle is expressed as[33]

$$F_{grad} = \frac{2\pi \nabla I_o \alpha}{c_o}, \tag{14}$$

where ∇I_o is the gradient of light intensity,

$$\alpha = 3V_p(\varepsilon_p - \varepsilon_m)/(\varepsilon_p + 2\varepsilon_m), \tag{15}$$

and c_o is the speed of light, while V_p is the particle volume, and ε_p and ε_m are the permittivities of the particle and suspending medium, respectively. The dielectric constant is a function of wavelength and is comprised of a real and an imaginary component, such that $\varepsilon = \varepsilon_1 + i\varepsilon_2$, where $\varepsilon_1 = n^2 - k^2$ and $\varepsilon_2 = 2nk$. n and k are the refractive index and absorption coefficient, respectively.[33] In the case of a simple, non-absorbing dielectric, α is positive when the

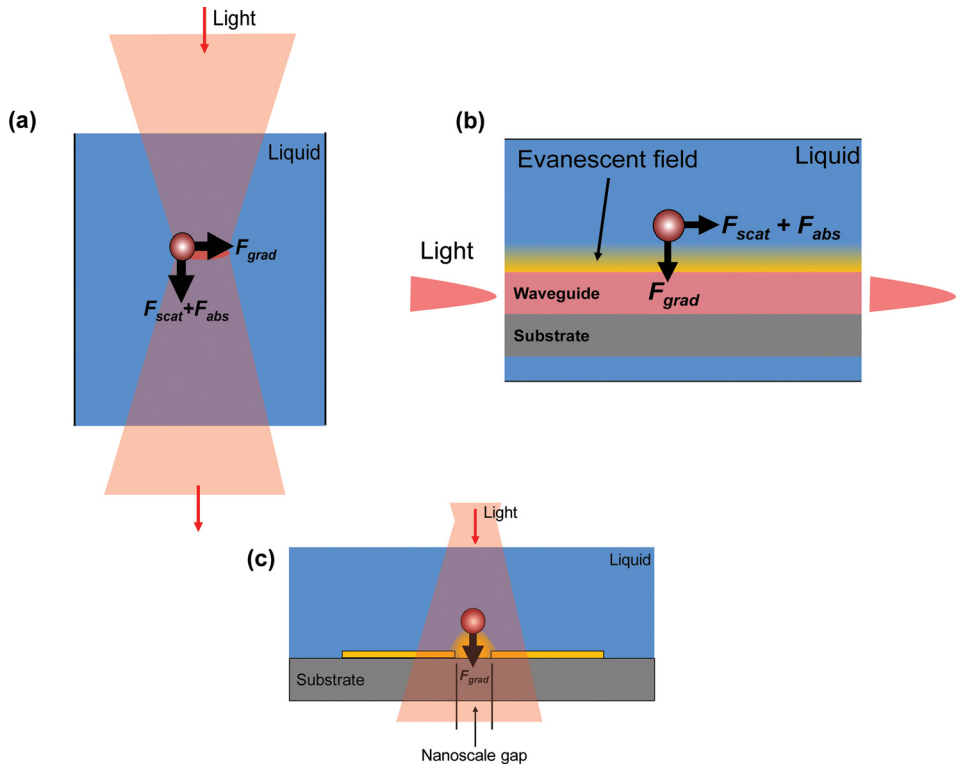

FIG. 6. Optical manipulation of suspended particles using (a) direct optical tweezing; (b) near field optical manipulation of suspended particles; (c) manipulation of particles using plasmonic nanostructures.

refractive index of the particle exceeds that of the surrounding medium. In this case, particles are attracted to the regions of highest intensity, and if the particles' refractive index is lower, it will be forced away from the regions of highest intensity.[33]

The scattering, F_{scat}, and absorption, F_{abs}, forces are expressed as[33]

$$F_{scat} = \frac{8\pi I_o \alpha^2 \varepsilon_m}{3 c_o \lambda^4}, \tag{16}$$

$$F_{abs} = \frac{2\pi \varepsilon_m I_o}{c_o \lambda} \mathrm{Im}(\alpha), \tag{17}$$

where λ is the optical wavelength.

Near-field manipulation refers to the optical manipulation of particles using evanescent fields.[33] When light travels through a waveguide, evanescent fields radiate from the waveguides' surface and decays exponentially with distance from the boundary of the waveguide where the optical wave originated.[81] The evanescent field generates a gradient force that attracts particles to the region of highest field intensity, before moving them under scattering and absorption forces, in the direction of wave propagation (Fig. 6(b)).[33]

2. Plasmonic manipulation

Plasmonic manipulation refers to the control of particle motion induced by surface plasmons.[82] Surface plasmons are electromagnetic waves produced by coherent electron oscillations at the interface of any two materials where the real part of the dielectric function changes sign across their interface.[83] The most suitable media are generally the boundaries of a metal and a dielectric material.[84] Surface plasmons are confined to the metal surface with exponentially decaying fields. In many applications, surface plasmons are generated by impinging light in the

visible range, although UV and infrared frequencies are also possible.[85] Surface plasmon resonances (SPR) refer to extremely large local enhancements of the electromagnetic field.[33] Plasmonic manipulation of particles can be achieved using either plasmonic particles or metallic nanostructures that support SPRs.

a. Plasmonic particles and their interactions. Plasmonic optical forces have been used to control particles composed of neutral dielectrics,[86] semi-conductors,[87] or metallic[88] structures. For SPR modes generated by plasmonic particles, naturally, particles need to be metallic or at least have a metallic shell. Plasmonic particles are particles that support localized surface plasmon resonances (LSPR). LSPRs have the ability to strongly scatter and absorb light and to squeeze light into nanometer dimensions, producing large local enhancements of electromagnetic fields.[89,90] LSPRs can be supported by a wide variety of metallic particles including interacting particle pairs, an array of particles with nano-scale gaps between them, or individual particles interacting with another metal surface. LSPRs can also be supported by nano-scopic holes or voids rather than particles, or by particles that have holes in them, such as toroidal structures.[85] Core-shell particles utilizing dielectric cores and metallic shells have also supported LSPR activity originating from the interaction of optical electromagnetic waves and the oscillating surface charges generated on the inner and outer surfaces of the metal shells.[91,92]

When light is incident on a metallic particle and the SPR conditions are met, the oscillating electric field of the light produces a force on the mobile conduction electrons in the metal, the result of which induces the LSPR modes.[85] The LSPR modes then generate a gradient force capable of particle trapping and manipulation. For example, the LSPR between a pair of closely spaced gold nano-dots were used to create an optical trap with improved particle positioning by reducing the trapping volume beyond the diffraction limit and quenching Brownian motion of the trapped nanoparticles by almost an order of magnitude as compared to conventional optical tweezers operating under the same trapping conditions.[93]

b. Plasmonic nanostructures and traps. Plasmonic nanostructures refer to metallic structures capable of producing SPR fields. An appropriately designed and patterned metal surface is required to provide plasmonic field confinement. Generally, the metallic structures are designed with nano-scale gaps between them where the SPR fields are produced.[85] Fig. 6(c) presents a plasmonic optical trap where a particle is held in place through the F_{grad} force, which acts to attract the particle to a surface bound metallic nanostructure.[33] Instead of using a highly focused laser beam (which is normally used in optical tweezing), surface plasmon-based optical traps as a result of plasmonic nanostructures enables stable particle trapping at a patterned metal surface even when using unfocused and low intensity laser beams.[82]

In summary, the optical manipulation of particles in microfluidic systems has been employed in order to achieve particle transport,[94] cell separation,[95] particle detection, and particle characterization.[96] The merits of this manipulation method include the ability of localizing light to the single particle level (particularly using plasmonic fields), being non-invasive and not requiring on-chip infrastructure, given that light can be sourced externally to the chip.[97] However, there is a risk of particle damage, especially with regard to organic entities, given that highly focused beams of light (in the case of optical trapping) can sometimes generate excessive heat.[98] Other disadvantages also include the requirement of bulk optics (in the case of far and near field manipulations), such as high numerical aperture objective lenses (hence large optical components), which impede the miniaturization requirements of certain devices.[82]

E. Magnetic

Magnetophoresis is the motion of suspended magnetized particles relative to a fluid under the influence of a non-uniform magnetic field.[99] Generally, the magnetic properties of materials can be classified into three categories: ferromagnetic, diamagnetic, or paramagnetic.[99] Diamagnetic materials are those whose electrons are all paired. The diamagnetic effect stems from changes in electron orbital motion induced by a magnetic field and leads to dipoles aligned

against the magnetic field.[99,100] Paramagnetic effects occur in materials whose electrons are unpaired and the spins of the unpaired electrons that align with the external magnetic field to produce a magnetic moment. Paramagnetism is exhibited when thermal fluctuations prevent the magnetic dipoles from locking in orientation aligned with the field. In contrast, ferromagnetism occurs in materials with unpaired electrons, when thermal fluctuations are small compared with the forces that lead magnetic dipoles to lock in orientation aligned with the field.[99]

When a particle is subject to a magnetic field, the force experienced by the particle, F_{mag}, is given by[39,100]

$$F_{mag} = \frac{(\chi_p - \chi_m)V_p}{\mu_o}(B \cdot \nabla)B, \tag{18}$$

where χ_p and χ_m are the magnetic susceptibilities of the particle and the suspending medium, respectively, V_p is the volume of the particle and μ_o is the permeability of free space ($4\pi \times 10^{-7}$ Hm^{-1}). The magnetic susceptibility refers to the degree of magnetization of a material as a result of an applied magnetic field.[101] If the particle is magnetic ($\chi_p > 0$) and the medium diamagnetic ($\chi_m < 0$), the difference of $\chi_p - \chi_m$ is positive, resulting in a positive value of F_{mag} and indicating the particle experiences an attractive force toward the regions of high magnetic flux density gradient (Fig. 7(a)). Conversely, when the particle is diamagnetic ($\chi_p < 0$) and the medium is paramagnetic ($\chi_m > 0$), the difference of $\chi_p - \chi_m$ becomes negative, giving a

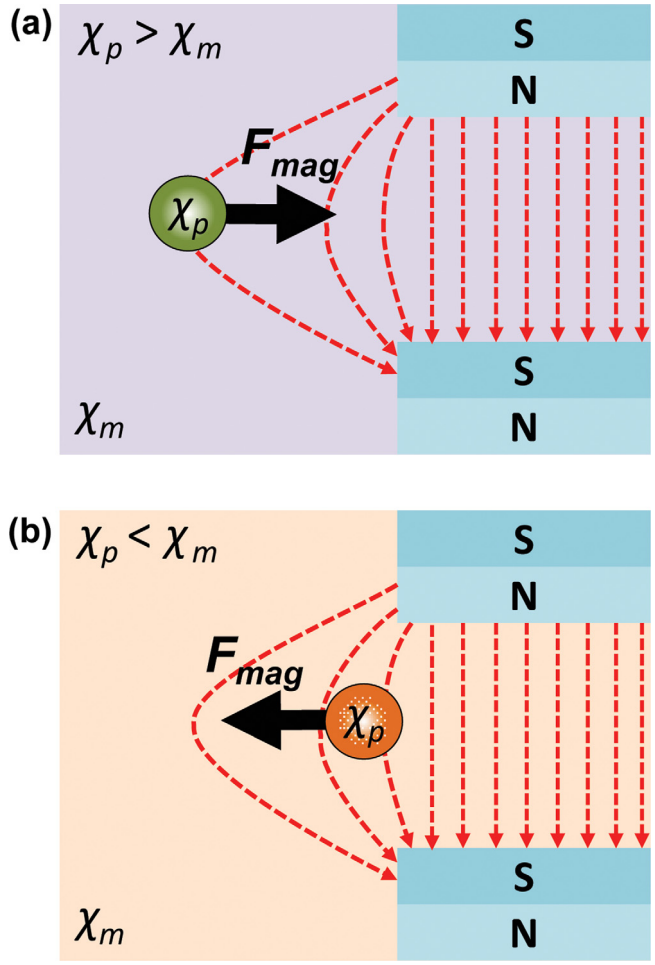

FIG. 7. Magnetophoretic manipulation of suspended particles. (a) Particle is pulled toward the region of high magnetic field gradients when $\chi_p > \chi_m$. (b) Particle is repelled from the region of high magnetic field gradients when $\chi_p < \chi_m$.

negative F_{mag} value signifying that the particle is repelled from the regions of high flux density gradient (Fig. 7(b)).[100]

Magnetophoretic manipulation has been used for particle separation,[102] sorting,[103–105] transport,[40,106] and detection.[107,108] Magnetophoresis has the advantage of angular particle positioning and rotation ability. It is minimally invasive and reduces the risk of particle damage in the process of particle control.[40] One of the problems associated with magnetophoresis involves the magnetic hysteresis of micro-particles, when the magnetic field is turned off, which can cause them to agglomerate into clusters. Smaller nano-scale particles however, display less hysteresis in the magnetic field, hence when the field is turned off, they redisperse in the suspension.[12]

III. APPLICATIONS OF OPTOFLUIDICS WITH SUSPENDED PARTICLES

In this section, we will describe novel optofluidic applications that have employed controllable particles suspended in liquid. First, applications of optical components which use particles as waveguiding media and lenses are covered. Subsequently, we describe optofluidic applications that have been used for transporting, detecting, and analyzing particles. Finally, we cover applications related to Raman spectroscopy, plasmonics, heat and energy and eventually those that specifically involve biological particles. The scope of applications reviewed is confined to optofluidic systems, which incorporate suspended particles. In particular, our focus is on such systems which utilize actively controlled particles.

A. Optical components

Multi-phase optofluidics have been used to create optical components that are compatible with liquids such as waveguides,[109] lenses,[110] and sensors.[111] However, a major setback of multi-phase systems is that liquids are not easily reconfigured and manipulated. One method of addressing this limitation is to use liquid with suspended particles. The properties of the suspension can be tuned from those of liquid to that of the particles by manipulating the particles concentrations at different locations within microfluidics. The concentrations of particles can be tuned using the externally applied forces described in Sec. II. In addition, the integration of suspended particles offers a wealth of added possibilities regarding the particles' interaction with light, which can be very useful for the development of particle detection and analysis platforms.[112]

1. Particles as waveguiding media

Several major works that have used controllable particles in realizing optofluidic waveguides will be briefed. The first was by Conroy *et al.*[113] The author demonstrated a particle core/liquid cladding waveguide, which uses two types of suspended particles, polysterene and SiO_2 with diameters ranging from 30 to 900 nm (Ø30 to Ø900 nm). Both particle types were focused using hydrodynamic forces (Fig. 8(a)). Visible light ($\lambda = 635$ nm) from an external laser source was coupled into the concentration of particles using a fiber embedded in the microfluidic channel. The output profiles showing the intensity of light guided through the particle focused core was observed (Fig. 8(b)). The analysis of core to cladding intensity ratios associated with the various particle sizes revealed that the smaller sized particle suspensions of higher concentrations guided light more effectively compared to the larger particles with lower concentrations. The authors attributed this to the smaller scattering cross sections exhibited by the smaller particles, when they were hydrodynamically focused. Additionally they suggested that suspensions with higher concentrations of particles had smaller inter-particle spacings and therefore the light experienced reduced scattering.

More recently, the major works by Kayani *et al.*[114] and Kalantar-zadeh *et al.*[115] demonstrated the use of DEP forces for the focusing and packing of suspended SiO_2 nanoparticles (Sizes: Ø230 and Ø450 nm). In their work, an array of curved DEP microelectrodes was used to generate a strong electric field gradient that traps the particles under a liquid flow, resulting

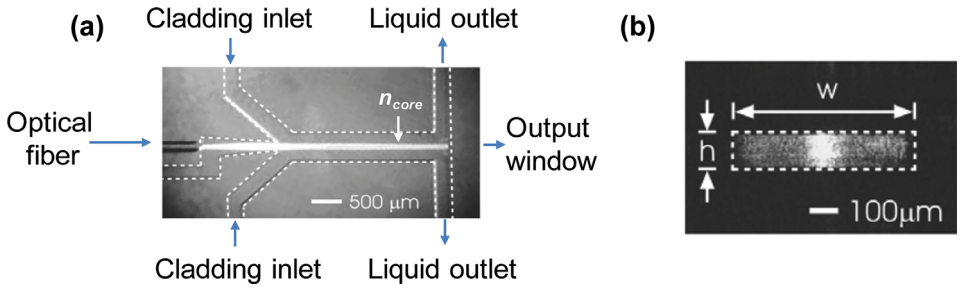

FIG. 8. Hydrodynamically focused nanoparticles used as optical waveguiding media. (a) Schematic of nanoparticle optofluidic waveguide using polysterene nanobeads and DI water, as the core and cladding, respectively. (b) Intensity distribution at the waveguide output showing a high core to cladding intensity ratio. Reproduced with permission from R. S. Conroy, B. T. Mayers, D. V. Vezenov, D. B. Wolfe, M. G. Prentiss, and G. M. Whitesides, Appl. Opt. **44**, 36 (2005). Copyright © 2005 American Chemical Society.

in the formation of particle dense narrowbands in the microfluidics. By focusing the particles, it was observed that the particle dense narrowbands in the center either scattered or guided the coupled light depending on their size and concentration.

It is worth noting that such particle enabled waveguides offer a number of advantages over purely homogenous liquid waveguides: (i) insoluble materials (such as suspended particles) can be used, (ii) refractive indices of core and cladding areas can be readily altered, and (iii) particles with a core-shell or crystalline structure can be optically/electrically/magnetically manipulated.[113] However, these particle based waveguides had practical issues such as the coupling of light through liquid inlets and outlets that induces major losses at the media interfaces and particle scattering.[114] To solve the scattering problem, Kayani *et al.*[9] demonstrated the coupling of light from a multimode rib polymeric waveguide to dielectrophoretically focused tungsten trioxide, WO_3 particles (Ø80 nm). When the particles were closely packed (Fig. 9(a)), there was a

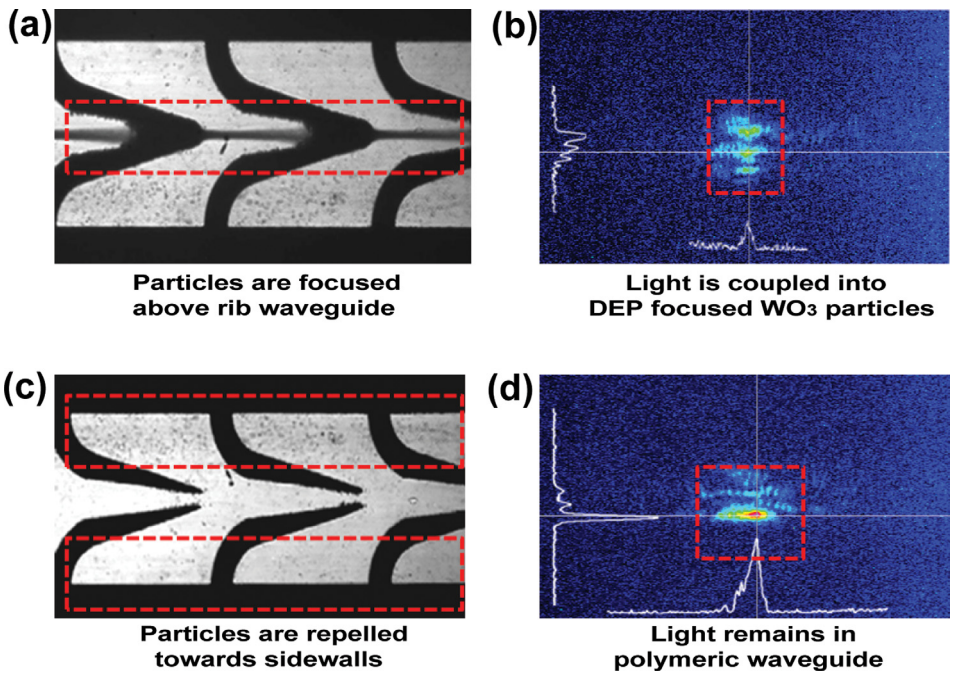

FIG. 9. Waveguide tuning using DEP focused particles. (a) WO_3 nanoparticles focused in the center of the DEP electrodes using positive DEP forces. (b) Light was coupled into the particle dense media above rib waveguide. (c) WO_3 nanoparticles repelled from the center. (d) Light remains in the polymeric rib waveguide. Reproduced with permission from A. A. Kayani, A. F. Chrimes, K. Khoshmanesh, V. Sivan, E. Zeller, K. Kalantar-zadeh, and A. Mitchell, Microfluid. Nanofluid. **11**, 1 (2011). Copyright © 2011 Springer Verlag.

strong interaction of the optical evanescent field of the rib waveguide with the DEP focused particles (Fig. 9(b)). Alternatively, when the WO_3 particles were repelled from the evanescent region of the rib waveguide (Fig. 9(c)), light remained guided in the rib waveguide (Fig. 9(d)).

2. Particles as lenses

Particles with suitable optical properties have been employed to focus light, similar to liquid lenses,[116] based on two different approaches: (i) particles can be individually used as lenses[117,118] and (ii) the accumulation of particles can be used to form particle arrays and media of different average refractive indices that could act as optical lenses.[119,120]

Individual particle lenses were demonstrated by several groups.[121,122] Such lenses have been used as manipulators of light exhibiting the ability to control the amplitude, phase, and polarization properties of light and its directions of propagation.[123–127] Beam control was demonstrated by displacing optically trapped particles such as an SiO_2 (Ø13 μm) microsphere through a light beam.[128]

Fig. 10 shows the schematic of the experimental geometry and simulation results of the particle light manipulation system using trapped SiO_2 particles. The microsphere caused the

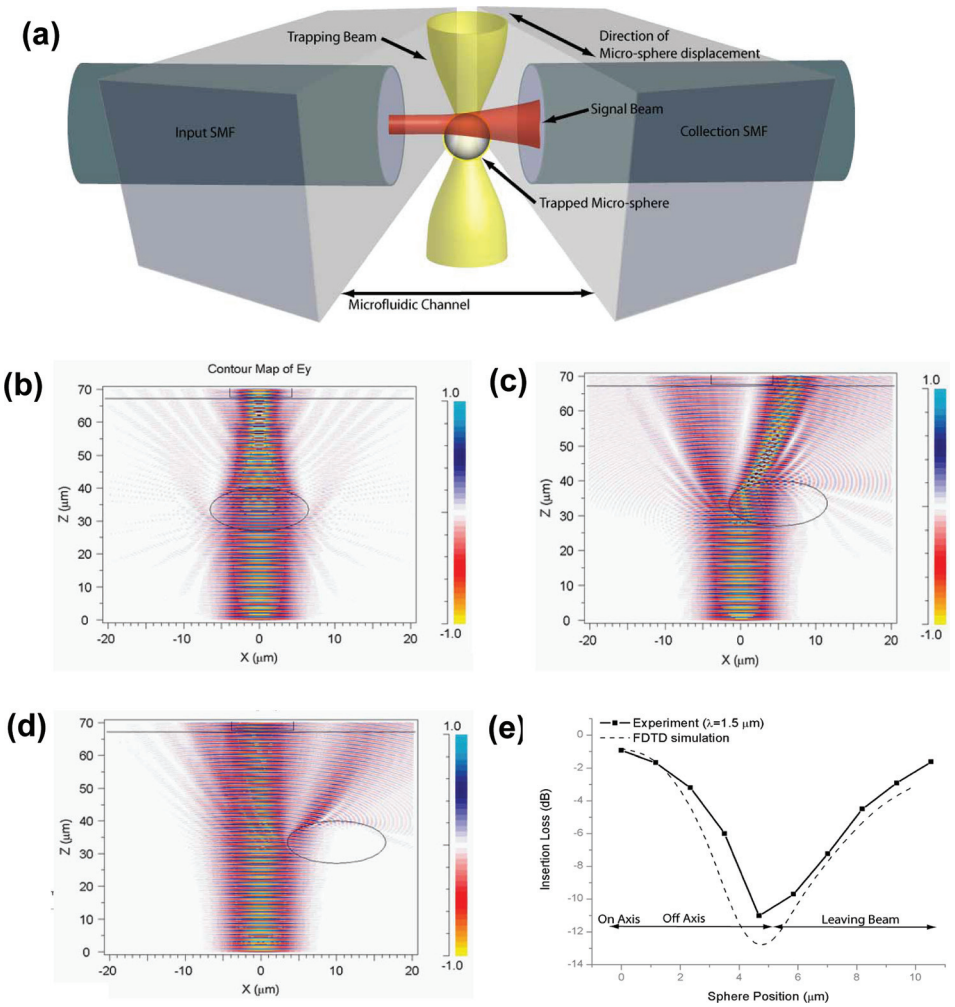

FIG. 10. Optofluidic lens using suspended particles controlled by optical forces. (a) Schematic of the experimental geometry for beam manipulation. FDTD field output depending on the microsphere position: (b) on axis, (c) off axis, (d) leaving beam. (e) Insertion loss experimental and numerical simulation data with transmission regimes are identified. Reproduced with permission from P. Domachuk, M. Cronin-Golomb, B. J. Eggleton, S. Mutzenich, G. Rosengarten, and A. Mitchell, Opt. Express **13**, 19 (2005). Copyright © 2005 American Chemical Society.

beam to be refracted by various degrees as a function of the particle position, providing tuneable attenuation and beam-steering in the device. The device itself consisted of the manipulated light beam extending between two buried single mode fiber (SMF) waveguides which were on either side of a microfluidic channel (Fig. 10(a)). This channel contained the microsphere, which was suspended in water. In the "on axis" transmission case, the microsphere was centered in the probe beam and acted as a spherical lens, providing enhanced coupling (Fig. 10(b)). In the "off axis" case, the microsphere steered the beam away from the core of the output SMF (Fig. 10(c)). In the "leaving beam" case, the microsphere was only slightly perturbing the probe beam, allowing most of the light to be collected (Fig. 10(d)). When the particle was located out of the center position, the signal intensity decreased to −11 dB compared to a continuous SMF case. Fig. 10(e) shows the experimental and numerical simulations of the insertion loss of the buried fiber device for various positions of the trapped microsphere, probed at a wavelength of 1.5 μm.

Accumulation of packed particles in microfluidics can also be used as optical lenses. For example, an optofluidic micro-lens was realized by filling a hollow fiber with ferrofluids consisting of suspended superparamagnetic iron oxide (Fe_3O_4) particles for the manipulation of light. The lens was constructed of a hollow fiber filled with superparamagnetic Fe_3O_4 nanoparticles (Ø10 nm) suspended in DI water at a 0.12% volume-in-volume (*v*/*v*) concentration. When the magnetic field was activated, the particles became aligned to the core surface such that it stretched the beam into a "ribbon shape" yielding a larger visible area and when the field was rotated, a larger beam spot size was formed. The ribbon shaped beam was formed by the diffraction of light incident on the particles in the fiber core.[4] In a separate work, the brightness and intensity of light was controlled with the aid of ferrofluids consisting of paramagnetic particles that were manipulated using magnetic fields on a magnetic film in a device known as an "optomagnetic dimmer."[129]

Other implementations of optical beam lensing or manipulation based on ferrofluids include the use of nickel nanorods produced by electroplating chemistry, which was shown to alter the shape of the laser beam passing through the suspension by varying the applied magnetic field.[130] The effect was caused by multiple scattering and diffractions of the laser beam due to the nanorods. It was established that magnetic nanorods (as opposed to spherical nanoparticles) are better suited for optofluidic beam illumination applications since they are more stable in a rotating magnetic field. In another example, Candiani *et al.*[131] demonstrated the use of ferrofluids and externally applied magnetic fields for manipulating optical beams transmitted in a hollow microstructured fiber integrated with Bragg gratings. The system was able to reflect optical wavelengths of light depending on the applied magnetic field while the magnetic particles acted as an in-fiber magneto-tuneable beam modulator.

The integration of controllable particles as optofluidic lenses has provided the ability to image large fields of view at high temperatures, free from the restraints of index-matching fluids, and it is expected to improve the sensitivity of microscopes and biological detectors and also have applications in other areas of biology and analytical chemistry in the future.[122]

B. Optofluidic platforms for particle transport

In the context of optofluidics, most particle transport examples use optical forces as described in Sec. II D. In this section, we will detail several novel examples of particle transport in optofluidic devices.

1. Transport of particles in liquid core waveguides

Particles can be transported in the core of waveguiding media using optical forces. In optofluidics, light in the core of waveguiding media can be confined by liquid and exerts optical forces that trap and transport the particles. One example of such devices is a photonic crystal fiber, which consists of a high index liquid core surrounded by a lower index periodic lattice of air capillaries. Mandal and Erickson[132] demonstrated the transport of polystyrene particles (Ø3 μm) using a liquid core photonic crystal fiber. In a separate work, polystyrene particles

(Ø1 μm and 3 μm) were shown to be drifted in a microfluidic channel using direct radiation of optical beams perpendicular to the fluid flow direction.[133] Light was focused into the microfluidic channel using on-chip lenses and their displacement in liquid was studied using various light focusing parameters.

2. Transport of particles using optofluidic waveguide near fields

As described in Sec. II D 1, the optical near fields can be used for transporting particles in microfluidics. An application example involves the field of a Y-shaped optical waveguide which transported polystyrene particles (Ø6 μm).[134] By shifting the position of the input fiber facet, power was directed to either side of the Y-branched output, which caused the particles to follow and be sorted on demand.

Another platform is the slot waveguide. A slot waveguide is an optical waveguide that strongly confines light in a sub-wavelength scale region, which is usually a low refractive index "slot" separated by slabs of high refractive index media.[135,136] The cavities in such slot waveguides can be filled with a liquid media and particles can be transported using such platforms as strong intensities and gradients of light occur in these slot cavities. Yang[137] investigated the trapping and transport of suspended polystyrene (Ø10 – 65 nm) and gold (Ø10– 65 nm) particles using silicon slot waveguides. The authors studied the effects of particle size, refractive index, and slot waveguide geometry on particle transport behavior. They also demonstrated the transport and trapping of λ-DNA molecules using such liquid core slot waveguides where the effects of varying slot widths were shown.[94]

Optofluidic ring resonators are another device that uses optical evanescent fields for particle transport.[138] In ring resonators, particles are attracted and propelled by optical forces along the evanescent field of a waveguide that branches into a ring structure. Due to the re-circulation of optical power in the ring, the optical power is significantly enhanced under certain resonant conditions.[139,140] The optofluidic ring resonators are highly suited for particle transport, separation, and sensing applications.[138,141,142]

Yang and Erickson[5] presented the transport of polystyrene particles (Ø3 μm) using an optofluidic ring resonator (Fig. 11(a)). The resonator structure was made of a polymeric waveguide. A portion of the optical power extends into the ring waveguide structure in the region where the distance between waveguide and ring is smallest. When the light that has travelled around the ring is in phase with incoming optical radiation, the optical waves constructively interfere resulting in a stronger optical field. The optofluidic ring resonator operates by alternating between an "on-resonance" and "off-resonance" state, which depends on the wavelength of coupled light. When the ring is "on-resonance," particles trapped on the bus waveguide will be routed to the ring due to optical gradient forces arising from stronger local field intensities in the ring (Fig. 11(b)). In the "off-resonance" state, the waveguide has a relatively stronger intensity (compared to the ring) and so the particles remain on the waveguide (Fig. 11(c)). Moving from the on-resonance to the off-resonance states and vice-versa is achieved by tuning the wavelength of the coupled light. Similar systems were shown by Cai and Poon.[143,144]

3. Transport of particles using optically induced virtual electrodes

Particles can be transported using a projection of virtual microelectrodes in a technique known as optically induced DEP manipulation or opto-electronic DEP tweezing. Chiou *et al.*[98] presented the manipulation and transport of suspended polystyrene particles (Ø4.5 μm) and cells using this method. The liquid containing the cells or particles of interest is sandwiched between an upper transparent, conductive glass, and a lower photoconductive surface. These two surfaces are biased with an AC signal. When the projected light illuminates the photoconductive layer, it turns the photoconductive substrate from behaving as an "insulator" to a "conductor" creating a non-uniform electric field gradient, which promotes particle transport and manipulation. Although such optically induced DEP devices are known to produce high resolution virtual electrodes, trapping of sub micrometer particles requires a large electric field gradient to overcome Brownian motion and therefore may require a higher powered optical source or bias for

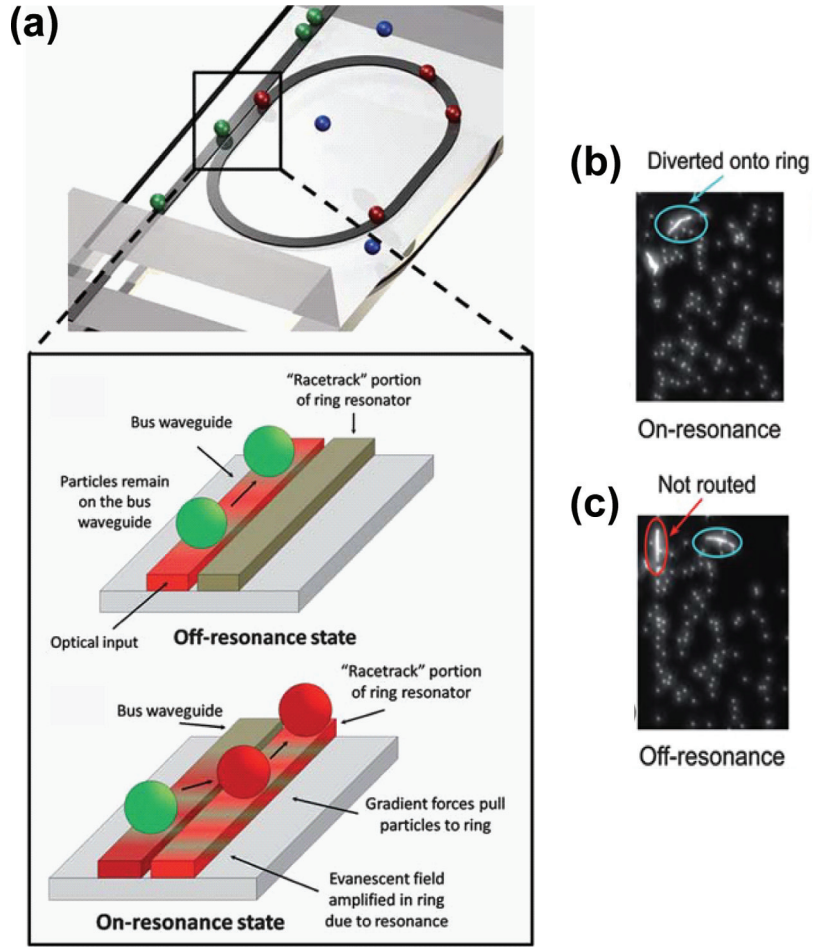

FIG. 11. Particle transport using an optofluidic ring resonator. (a) Schematic of optofluidic ring resonator switch with boxed figure showing the switching mechanism due to optical forces when the ring is strongly coupled at the resonant wavelength. (b) Trapped particles are diverted and continue to move forward on the ring under the on-resonance state. (c) In the off-resonant state, particles pass through the switching junction and are not routed into the ring structure. Reproduced with permission from A. H. J. Yang and D. Erickson, Lab Chip **10**, 6 (2010). Copyright © 2010 The Royal Society of Chemistry.

generating the required translational force. The virtual electrodes generated are not directly used for particle trapping, and instead trapping performance is achieved *via* the re-distribution of the applied AC potential between the fluids and the substrate. Such optically induced DEP platforms are advantageous as they produce high optical powers and the small pixel sizes of the virtual electrodes result in highly dynamic and accurate particle displacements.[145,146]

4. Transport of particles using holographic optical tweezers and the optical stretcher

Recently, optical tweezers have been transformed by the availability of spatial light modulators and the speed of low-cost computing that drive them. Holographic optical tweezers have the ability to trap and move many suspended particles simultaneously and their compatibility with other optical techniques, particularly microscopy, means that they are highly appropriate for lab-on-chip systems to enable optical manipulation, actuation, and sensing.[147] Various approaches for the generation of optical beams that combines established techniques of holographic optical trapping with hollow intensity distributions have allowed the simultaneous stable trapping of multiple particles at defined pre-defined positions.[148,149]

The optical stretcher is a novel, dual-beam optical trap that is capable of trapping and stretching dielectric particles, such as living biological cells, along the beam axis. Unlike

conventional optical tweezing, which use a single focused beam to produce a point like trap, the optical stretcher uses diverging light spread across the particle surface. The unique features of the optical stretcher is that the optical force is applied at all points along the particle surface as opposed to at the center of the particle mass and that it is able to exert pico-Newton scale surface forces on the living cell without making mechanical contact.[150] Additionally, since no optical beam focusing is required, the optical stretcher is known for producing minimal radiation damage and hence is highly suitable for characterizing and even manipulating biological particles and cells.[151]

C. Optofluidic devices for particle detection and analysis

In this section, we describe optofluidic devices that have been used for detecting and analyzing particles. In such devices, generally, particles are transported using the manipulation forces (described in Sec. II) and then they are passed through an optical interrogation or excitation region, where they are detected and analyzed.

1. Detection based on fluorescence and light scattering

Fluorescence detection has been used in many areas, particularly bio-applications, by incorporating particles that show fluorescence emissions.[10] They are used as the labels for revealing the presence and tracing the movement of such particles. Light scattering is another method of detecting and analyzing particles. The analysis of scattered light allows the determination of particle characteristics such as size, refractive index and absorption coefficient.[152] Therefore, relevant information about a particle can be inferred from the analysis of the scattered light.

There are many examples of optofluidic applications that incorporate fluorescent particles. Perroud *et al.*[153] demonstrated the identification and sorting of macrophage cells based on fluorescent signals. Shi *et al.*[54] presented the fluorescent detection and tracking of polystyrene (Ø0.87 μm and 4.16 μm) beads in a microfluidic channel. Parallel inter-digitated acoustic resonators were used to position and separate the particles so that they could be sorted into three fluidic outlets. Fluorescence spectroscopy was then used to track the separation of the particle types.

There are also many examples of analyzing particles based on scattering methods. Mitra *et al.*[154] demonstrated the detection, sorting and size characterization of viruses and particles using an optofluidic interferometer. The detection scheme used was able to detect and sort single viruses and also distinguish different kinds of virus types in a mixture of viruses.

2. Optofluidic anti-resonant reflecting optical waveguide platforms

The hollow core anti-resonant reflecting optical waveguide (ARROW) is often used for guiding light in liquid, particularly in microfluidic systems.[155] ARROWs can be formed by a low index core layer, which is embedded between higher index layers. This addresses the difficulty of finding suitable optical cladding materials, with a lower refractive index than liquid, making them well suited for optofluidic applications. ARROW platforms have the advantage of low loss of signal, almost single-mode behavior and they have high polarization selectivities.[156]

The fabrication and operation of ARROW waveguides have been well documented.[111] An example by Measor *et al.*[6] is demonstrated in Fig. 12. It is an optofluidic ARROW platform that provides a perpendicular excitation and detection geometry and that caters for sensitive particle and bio-molecular detection applications. The device was made of a high refractive index layer surrounding a hollow core filled with the suspended particles that needed to be analyzed (Fig. 12(a)). Light that is coupled into the solid-core ARROW waveguide (Fig. 12(b)) provides an optical excitation to the fluorescent labelled particles that flow through the hollow core waveguide (Fig. 12(c)). The hollow core waveguide is filled with liquid and the particles that flow through the hollow core are transported using dual beam optical trap. The ARROW platform has been used for detecting liposomes, DNA fluorophores, and viruses.[111,157–160]

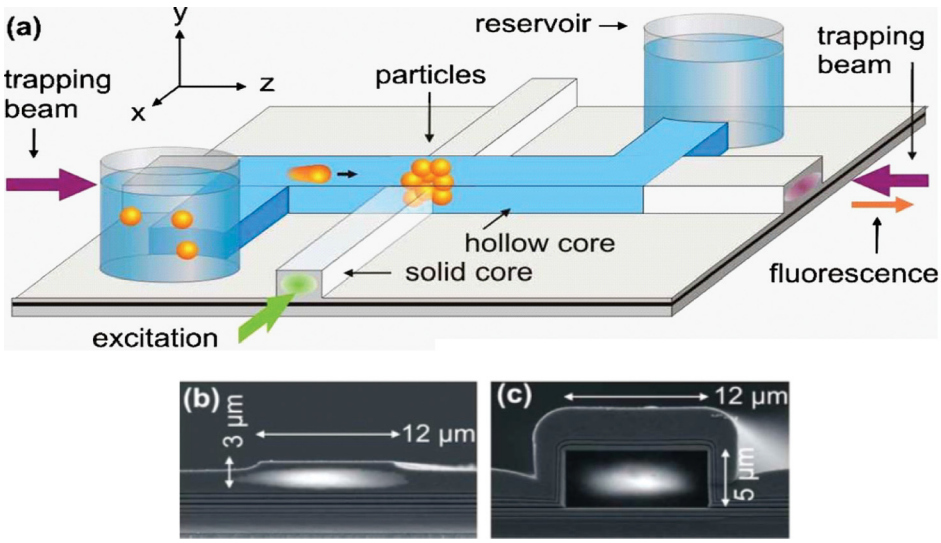

FIG. 12. Optofluidic ARROW platform optimized for particle detection. (a) Schematic of the integrated optofluidic system with perpendicular excitation/collection geometry for detecting bio-molecules (b) SEM images of solid core and (c) liquid core ARROW waveguide cross-sections. Reproduced with permission from P. Measor, B. S. Phillips, A. Chen, A. R. Hawkins, and H. Schmidt, Lab Chip **11**, 5 (2011). Copyright © 2011 The Royal Society of Chemistry.

3. Optofluidic flow cytometers

The flow cytometer is perhaps one of the most important optofluidic detection platforms, as it provides *in situ* cell counting, fluorescence detection and cell sorting, all in an integrated device. This device provides fast quantification of different organic and inorganic particles and cells. Generally, the sample containing the particles is hydrodynamically sheath focused by a surrounding buffer liquid to obtain a stable particle line-up. The particles then pass through an optical interrogation region, where they are detected and characterized based on their fluorescence emissions and scattering of light.[161]

Shvalov *et al.*[152] presented one of the earliest versions of the flow cytometer that was able to distinguish lymphocytes, erythrocytes, and polystyrene particles of various sizes and refractive indices. The analysis of particles was conducted by examination of the unique profiles of scattered light that had varying scattering angles from the particles. Steen[162] also presented the earlier version of the cytometers capable of detecting viruses of various sizes ranging from 70 to 300 nm.

Today, flow cytometry has evolved tremendously. Although fluorescent detection and hydrodynamic forces are conventionally used, new methods such as impedance detection is being integrated into microflow cytometers for microparticle-based assays and magnetophoresis of biomolecules is being used for particle sorting.[163] Modern cytometers also feature optofluidic liquid lenses that focus light into the particle interrogation region for more effective particle analysis.[164] Zhu *et al.*[165] presented a compact and cost-effective cytometer, for resource limited regions, integrated with cellular phone imaging. In this device, fluorescently labelled particles were continuously delivered to an imaging volume *via* a disposable microfluidic channel. The videos were captured by the cellular phone camera and analyzed for particle/cell counting. Such platforms could be useful for rapid and sensitive imaging of bodily fluids and for conducting various cell counts and analysis as well as for screening of water quality in remote and resource-poor settings.

Flow cytometers have also been integrated with DEP microelectrodes for the sorting and characterization of cells such as yeast.[166] In this work, positive DEP forces were used to sort between viable and non-viable yeast cells. This was possible as viable and non-viable yeast cells were found to have different DEP spectral behavior so they could be sorted by these properties before being counted. After passing through the "DEP filter" region, light scattered from the specimens was collected by an integrated waveguide and analyzed.

D. Raman spectroscopy of particles

Raman spectroscopy (RS) provides analytical information about a sample's molecular structure and composition[167] and has attracted considerable attention due to its high sensitivity and low detection limits in sample detection. RS is a spectroscopy technique that relies on the inelastic scattering of monochromatic light from a sample.[168] A small portion of light scattered from the sample is scattered at a series of different wavelengths that are indicative of the vibrational transitions of the molecules.[169] Because different molecules have different vibrational modes, the spectrum of the inelastically scattered light uniquely identifies the sample. Surface enhanced Raman spectroscopy (SERS) is a surface-sensitive technique that enhances the Raman scattering signal by molecules adsorbed on rough metal surfaces.[168] In SERS, the target molecule is brought into close proximity to a metallic (typically Ag, Au or Cu) surface with nanoscopically defined features or in solution of such metallic nanoparticles with feature sizes smaller than the wavelength of the excitation light. When light is incident on the surface or particle, a surface plasmon mode is excited, which locally enhances the electromagnetic energy in the vicinity of the target molecule, significantly enhancing the intensity of the inelastically scattered light. The total enhancement to the Raman signal observed in response to this effect can be several orders of magnitude larger than that of the unenhanced Raman signal.[169]

In microfluidic systems, the particle characterization process using RS analysis can be complex. The sensitivity of the Raman signal needs to be high but yet the challenge lies in developing a stable and reproducible Raman-active substrate under constant liquid flow. Also, it is complicated due to the non-uniform distribution of the SERS-active substrates when they are dispersed in liquids. One of the solutions to these underlying issues is to employ controllable particles. Particle manipulation forces that have been employed for controlling particles as SERS-active targets in the microfluidic-RS devices include hydrodynamic, dielectrophoretic and optical forces.

Wang *et al.*[170] demonstrated an optofluidic SERS device that uses a pinched and step microchannel junction to trap and assemble nanoparticles/target molecules into optically enhanced SERS active clusters under hydrodynamic capillary forces. Chrimes *et al.*[171] demonstrated optofluidic SERS measurements (Fig. 13(a)) with the aid of DEP microelectrodes for the mapping,

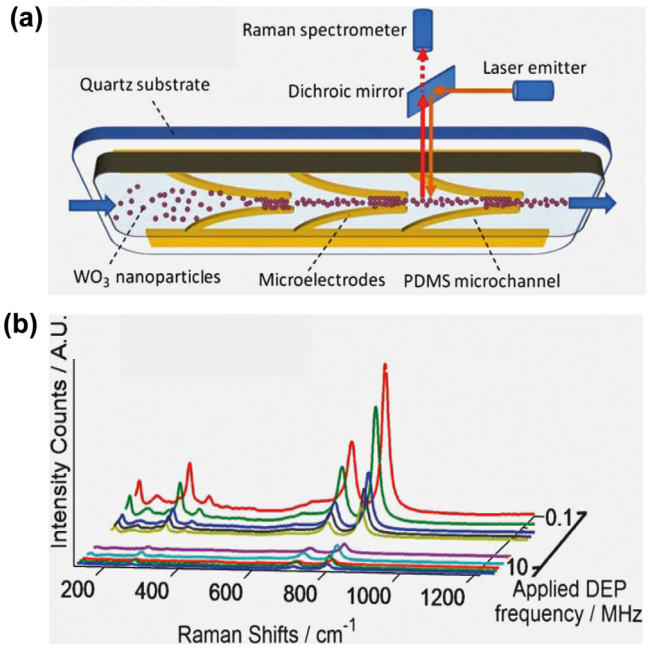

FIG. 13. Raman spectroscopy analysis using a DEP microfluidic platform. (a) Schematic of DEP-Raman system layout. (b) Plot of WO_3 nanoparticle Raman spectra at different DEP frequencies, decreasing in frequency along the *z*-axis. Reproduced with permission from A. F. Chrimes, A. A. Kayani, K. Khoshmanesh, P. R. Stoddart, P. Mulvaney, A. Mitchell, and K. Kalantar-zadeh, Lab Chip **11**, 5 (2011). Copyright © 2011 The Royal Society of Chemistry.

recognition, and concentration measurement of WO_3 nanoparticles (Ø80 nm, $n = 2.3$). A curved DEP microelectrode array concentrated the moving particles at the SERS detection region. When the particles were concentrated to the region between the electrodes, the Raman spectral peaks were higher, indicating a higher concentration of particles. It was revealed that reducing the DEP frequency with a constant magnitude signal would increase the concentration of particles in between the curved electrodes. Fig. 13(b) presents the Raman spectral peaks as a function of DEP applied frequencies. It shows that as the DEP applied frequency is reduced, particle concentration increases and thus the Raman spectral peaks are amplified. This platform enables *in situ* analysis of particles flowing in liquid, without the need for dehydration or immobilization as in conventional SERS devices. They applied this concept for the active control of the nanoparticles spacing to increase the SERS signal intensity based on augmenting the number of SERS-active hot-spots. The superb capability of the system was demonstrated by detecting dipicolinate (2,6-pyridinedicarboxylic acid), which is a biomarker of *Bacillus anthracis* at 1 ppm.[172]

White *et al.*[173] used optical gradient forces from the evanescent fields of optofluidic ring resonator waveguides to enhance SERS-detection where light was confined within the high refractive index liquid core of the waveguide. Rhodamine 6 G mixed with silver particles (Ø50-100 nm) formed nanoclusters and were used as the target sample in the experiments. The liquid core optical ring resonator serves both as the microfluidic sample delivery mechanism and as a ring resonator, exciting the metal nano-clusters and target analytes as they pass through the channel. Tong *et al.*[174] demonstrated the use of optical and hydrodynamic forces to aggregate Ag particles (Ø40 nm) in the Raman-detection region. Thiophenol (TP) and 2-naphthalenethiol (2-NT) were adsorbed to the Ag particles to form the target sample. In a separate work, cell transport and sorting was achieved using a combination of hydrodynamic and optical forces while a RS signal was used for both, identification and simultaneous sorting of label-free leukemia cells.[175] Such platforms are suitable for automated particle identification and sorting.

The ARROW platform, described in Sec. III C 2, has also been used for SERS detection. The high optical intensities of light that propagate along the liquid core of the ARROW waveguide were used to trap the target Rhodamine 6 G molecules that were adsorbed to the Ag particles. The enhanced RS signal was able to detect the molecules at a low dispersion concentration of 30 nM.[176]

E. Plasmonic inspired optofluidics

In this section, we focus on describing optofluidic devices, which incorporate both plasmons and suspended particles. The applications of such optofluidic devices are mostly found in areas of particle manipulation[177–180] and sensing.[88,181] Commonly in many plasmonic measurements and manipulations, metal (such as gold or silver) nanostructures or nanoparticles are used to provide the enhancement for surface plasmons. The systems are either based on prefabricated nanostructured surfaces (such as surfaces with arrays of nano-posts and nano-roughened surfaces) or agglomerated nanoparticles. Nanostructured surfaces or agglomerated nanoparticles show significant hot-spot enhancement when grains or particles form optimum spacing in the order of several to tens of nanometers.[182]

1. Plasmonic transport of particles

We described the features and advantages of plasmonic manipulation of particles in Sec. II D 2. A good example is demonstrated by Wang *et al.*[183] They used surface plasmons generated on a gold stripe in order to manipulate transport polystyrene (Ø1–2 μm) particles in a microfluidic channel (Fig. 14(a)). The particles were moved using optical forces, which resulted from the SPR excitations of light in close vicinity of the gold stripe. Fig. 14(b) shows the images of scattered light, which gives an indication of the particles' locations for analyzing their motion and velocity.

Plasmonic transport was also demonstrated using an array of gold micro-pads that acts as plasmonic traps using a visible laser to provide the SPR excitations.[179] In this work, polystyrene (Ø5 μm) particles and yeast cells were manipulated and trapped in close vicinity of the micro-pads, where the optical intensity gradients were high. In a separate work, the transport of

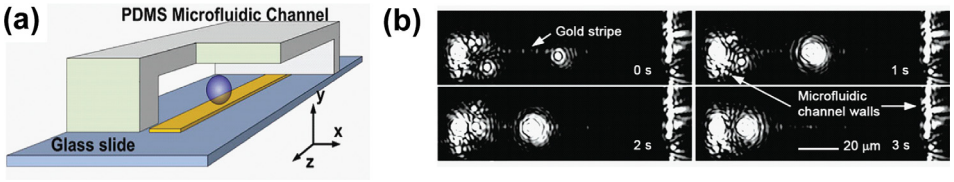

FIG. 14. Optofluidic device used for plasmonic transport of particles. (a) Schematic of optofluidic-plasmonic trapping device, consisting of a gold stripe in a microfluidic channel formed on a microscope glass slide. (b) Time sequence of scattered light images of particles in the microfluidic channel. Adapted from Ref. 183.

polystyrene (Ø6 μm, 1 μm, and 200 nm) particles was demonstrated near the surface of gold nano-structures (~130 nm diameter gold nano-dot pairs separated by a gap of 200 nm).[93] When the laser excitation source was moved, the SPR fields close to the nano-dot array moved the particles as well.

2. Plasmonic sensing

SPR technology has been rapidly gaining acceptance as an advanced and reliable sensing technique.[184–186] This technique has the advantage of high sensitivity to refractive index changes, label free detection, and it reduces the need for fluorescent binding of the target analytes.[169] A surface plasmon is excited by a light wave propagates along a metal film, and its evanescent field probes the target particle nearby. A perturbation in the refractive index of the target gives rise to a change in the surface plasmon characteristics. These characteristics include the coupling angle, coupling wavelength, intensity, and phase of the light.[184,187]

A good example is the work of Hsu *et al.*[188] They demonstrated a plasmonic sensor using a partially unclad optical fiber with gold (Ø16 nm) and silver (Ø32 nm) particles attached to the waveguide core surface. The unclad fiber was placed in the flow direction of a microfluidic channel to enable the delivery of target analytes by hydrodynamic forces. The detection and identification was based on the analysis of evanescent-wave absorption of the metallic particles located on the fiber surface. The plasmonic bio-sensor was able to detect streptavidin, dinitrophenol, ovalbumin antigens, and matrix metalloproteinase-3 genes at low detection limits.

F. Thermal and energy related applications

1. Thermal

In this section, we describe thermal and energy related applications of optofluidics, which incorporate controllable particles. Thermally induced particle motion stands as the main kinetic process involved in "thermo-optofluidic" applications. In these applications, particles are generally heated, causing them to migrate according to thermophoretic behavior that was described in Sec. II C.[189,190] Sources of heat can be optical, mechanical, or electrical. It has also been demonstrated that certain plasmonic nanostructures[191] and thermally responsive particle composites[192] absorb and induce localized heating upon exposure to light.

Duhr and Braun[193] demonstrated the thermophoretic transport of DNA molecules. In this work, the tracing of the DNA molecule concentrations were recorded by fluorescence measurements. In a separate work, a focused beam of near-infrared light was used to induce heat and manipulate polystyrene (Ø49 and Ø100 nm) particles which were also fluorescently labelled for tracking purposes.[194]

Baaske *et al.*[195] demonstrated the thermophoretic manipulation of aptamer bindings consisting of human blood serum (Fig. 15). In this work, the blood serum inside a microfluidic capillary was locally heated using a focused infrared laser (Fig. 15(a)). The aptamers motion in response to the locally generated heat was traced using fluorescence spectroscopy. When the laser was turned on, the aptamers moved away from the heated spot and when the laser was turned off, the aptamers diffused back (Fig. 15(b)). The authors also used the device to quantify the biomolecular binding reactions of unlabelled aptamers to the target blood serums.

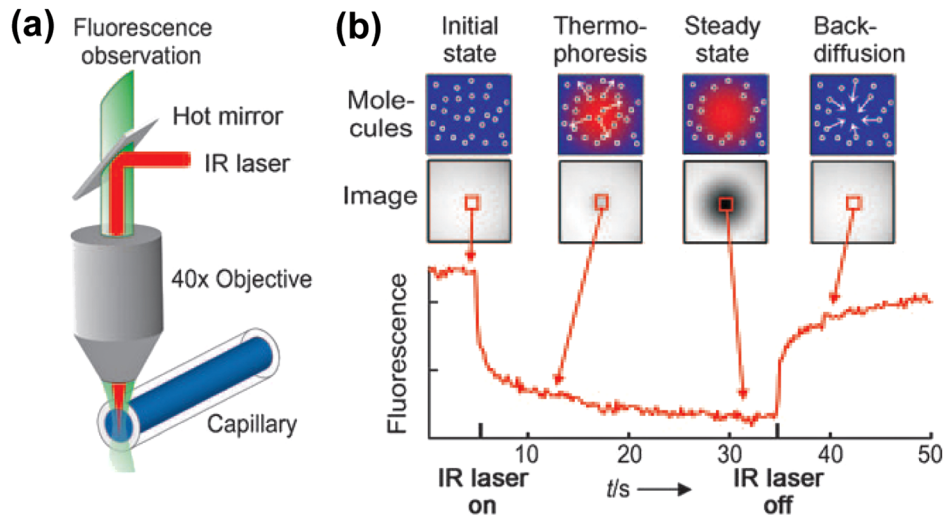

FIG. 15. Thermophoretic transport of aptamer bindings: (a) The blood serum inside the capillary is locally heated with a focused IR laser, which is coupled into an epifluorescence microscope using a heat-reflecting "hot" mirror. (b) The fluorescence inside the capillary is imaged with a CCD camera, and the normalized fluorescence in the heated spot is plotted against time. The IR laser is switched on at $t = 5$ s, the fluorescence decreases as the temperature increases, and the labeled aptamers move away from the heated spot because of thermophoresis. When the IR laser is switched off, the molecules diffuse back. Reproduced with permission from P. Baaske, C. J. Wienken, P. Reineck, S. Duhr, and D. Braun, Angew. Chem., Int. Ed. **49**, 12 (2010). Copyright © 2010 John Wiley and Sons.

2. Energy generation

Recently, a review by Erickson *et al.*[196] described the potential opportunities in optofluidics research involving fuel production using photo-bioreactors and photo-catalytic systems. Also, the author described optofluidic enabled solar energy collection and control.

Basically, the authors presented the opportunity of enhancing solar-energy based fuel production using photo-bioreactors containing photo-catalytic particles such as TiO_2 in microfluidics. It was argued that these reactors could harvest optical energy generating entities such as oil, hydrogen, and isobutanol from microorganisms. The second point presented was the conversion of water into its hydrogen and oxygen components, and the conversion of carbon dioxide and water into hydrocarbon fuels using photo-catalytic reactions of micro- and nano-particles.

G. Optofluidics incorporating biological particles

Optofluidics research has had a remarkable impact on the life sciences field. Biological particles such as proteins, DNAs, organelles, cells, and other microorganisms have all been used and incorporated in optofluidic devices. In previous sections, we mentioned some of the applications of bio-particles to highlight their relevant optofluidic properties, particularly in Secs. III C and III D. However, we exclusively devote this section to bio-particles used in optofluidic systems, which have not been discussed previously.

The use of bio-particles in optofluidics can be divided into two major categories: (i) Optofluidic devices used for the analysis and transport of bio-particles such as filtering and sorting and (ii) Optofluidic devices enabled with bio-particles such as organic lasers. We focus on describing novel applications of such "bio-enabled" optofluidic devices with the emphasis on particles that are controlled by externally applied forces.

1. Optofluidics for the transport and analyses of biological components

There have been many applications of optofluidic devices being used for transporting and analyzing bio-particles. These particles were manipulated using a variety of forces such as magnetic, acoustic, and optical forces.

Many optofluidic systems use the magnetic properties of particles for eventual bio-applications. An example of such manipulation is presented in the work of Lien *et al.*[197] They used antibody conjugated magnetic beads (Ø4.5 μm) to detect and isolate influenza A viruses. Target influenza A virus, which was immobilized onto the surface of the magnetic beads. This was followed by labelling the fluorescent signals onto the virus-bound magnetic complexes and analyzing them using an optical detection module. Another optofluidic bio-analysis platform involves a multi stage separation system that separated a cell mixture in blood based on their magnetic susceptibility properties.[198] The platform separated red and white human blood cells using the magnetophoretic force while fluorescent imaging was used to trace the particle separation efficiencies.

Lenshof *et al.*[199] reported an acoustophoretic manipulation platform that isolated plasma from whole blood. The acoustophoretic separator could remove enriched blood cells in multiple steps to yield high quality plasma with a low cellular content. Based on fluorescence measurements, the plasma had erythrocyte concentrations of less than 6.0×10^9 units and a low concentration of prostate specific antigens.

Optical forces can exert force on bio-particles as described in Sec. II D *via* either far or near field. In one example, Hwang *et al.*[200] demonstrated the separation of *oocytes* (cell in the reproduction system produced by the human ovaries) in an optofluidic platform based on optically generated virtual electrodes for *in vitro* fertilization. The device was successful in separating the fertilizable and abnormal *oocytes* from the mixture based on their responses toward the generated optical fields and their motion velocity differences (Fig. 16). Kim *et al.*[201] demonstrated an optofluidic device, which consists of a microchannel and an optical waveguide structure inside fused silica for the interrogation and processing of single cells. Single red blood cells in diluted human blood moving inside a microchannel were detected by the intensity change of the light delivered by the waveguide.

Plasmonic optical manipulations of bio-particles in microfluidics are great examples of near field forces on such particles. Biological particles were trapped using plasmonic induced forces. For example, Righini *et al.*[202] demonstrated the trapping of living *Escherichia coli* bacteria for several hours using moderate light intensities. The control of bacteria was achieved using metallic nano-antennas patterned on a glass substrate to produce strong light intensity gradients when illuminated by a resonant optical source.

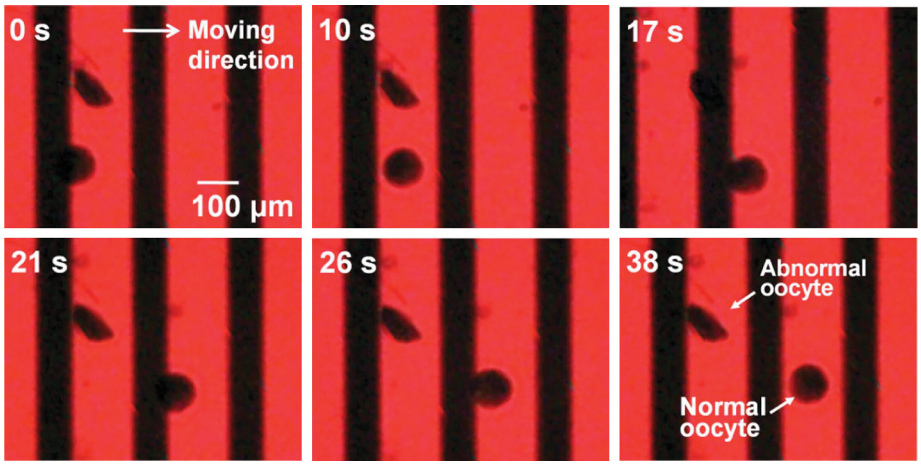

FIG. 16. Captured images of the discrimination of normal and abnormal *oocytes* using an optically induced DEP electrode scanning from left to right. Samples were manipulated at the DEP voltage of 10 V_p at 1 MHz. When the DEP signal was applied and the projected DEP electrodes were moved, only the normal *oocyte* were displaced in the direction of image pattern, while the abnormal *oocytes* remained at the initial position. Reprinted with permission from H. Hwang, D.-H. Lee, W. Choi, and J.-K. Park, Biomicrofluidics **3**, 1 (2009). Copyright © 2009 American Institute of Physics.

TABLE I. Summary of particle manipulation methods, features, limitations, and references.

Manipulation technique	Features	Limitations	Key references
Hydrodynamic	• Influenced by hydrodynamic drag force and governed by laminar flow regime • Sheath and sheathless focusing of particles extensively used • Depends on particle size, viscosity, and flow rates of the fluids	• Extensive fluidics simulation and design of microchannel required • Small changes in microchannel dimensions alters particle motion trajectory • Sensitive to flow rate changes	Xuan *et al.*[42] Squires *et al.*[45] Tanyeri *et al.*[48]
Acoustic	• Acoustic waves exert acoustic forces on particles in liquid • Capable of particle separations based on size, density, and compressibility • Depends on magnitude and frequency of the acoustic wave, size, and elasticity of the particle and surrounding liquid	• Difficulty integrating micro-scale bulk acoustic wave resonators into microfluidic structures • Ineffective manipulation accuracies for nano-scale particles • Differentiation of particles by size, density, and compressibility differences only	Friend *et al.*[27] Shi *et al.*[54] Petersson *et al.*[50]
Electrophoresis	• Control of charged particles using uniform electric fields • Electrophoretic force induces motion of the charged particle towards the opposite charge electrode • Depends on permittivity and size of the particle and viscosity of the suspending medium	• Generally limited to purification and separation applications • Slow particle migration times • Limited to charged particles	Gas[32] Kleparnik[31] Melvin[59]
Dielectrophoresis	• Control of neutral/semiconducting particles in non-uniform electric fields • Motion depends on relative polarizabilities of the particle with respect to surrounding medium • Depends on particle size, permittivity, and conductivity of the particle and suspending medium	• Motional accuracies limited by the performance of the DEP electrodes • Reduced particle sizes severely reduced magnitude of DEP force • Risk of bio-particle damage when subjected to high electric field gradients	Zhang *et al.*[28] Kuzyk[66] Khoshmanesh *et al.*[30]

TABLE I. (*Continued*.)

Manipulation technique	Features	Limitations	Key references
Thermal	• Observed when a temperature gradient is applied to particles suspended in liquid • Used for particle separation and migration and motion based on particle thermophobicity or thermophilicity properties • Depends on particle concentration, thermal diffusion coefficient, and temperature gradients	• Difficult to transport particles individually as particles move in clusters • Generally motion is from hot to cold regions (particles thermophobic) • Typically slow particle drift times	Piazza *et al.*[67] Plyukhin *et al.*[69] Parola *et al.*[35]
Optical	• Classified as either direct tweezing, near-field, or far field manipulation • Extensively used in particle transport, sorting, and characterization • Depends on particle size, volume, permittivities of particle and suspension, optical wavelength, and intensity gradients	• Extensive optical peripherals required for implementations • Generates excessive thermal heating due to high intensity optical beams • Generally not suitable for bio-particles due to risk of damage arising from heat absorption from optical waves	Jonas *et al.*[34] Erickson *et al.*[33] Halas *et al.*[84]
Magnetic	• Motion of particles subject to magnetic field gradients • Ability to induce angular rotation of particles, it is minimally invasive and generally safe for bio-particles • Depends on magnetic susceptibilities of the particle and suspending medium, particle volume, and the applied magnetic field gradients	• Agglomeration of magnetic particles and hysteresis in on/off magnetization sequence • Limited to particles that are magnetic or have some magnetic content • Non-magnetic particles have to be chemically bound to magnetic particles which can be complex	Suwa *et al.*[38] Ivon Rodriguez-Villarreal *et al.*[100] Peyman *et al.*[39]

2. Optofluidics enabled with biological components

Optical components such as lasers have important applications ranging from optical communications and medicine to materials processing and analysis. In order to tailor the properties of light emitted by lasers to the specific needs of each application, different optical gain materials are required. Until recently, however, little work has been done on using bio-particles in microfluidics as part of the "lasing medium" of lasers.[203]

Lasers based on particles in microfluidics generally fall in the category of dye lasers. Dye lasers are generally wide bandwidth. The wide bandwidth range makes the dye lasers particularly suitable for tuneable and pulsed laser applications. Dye lasers are commonly used in medical spectroscopy, biochemical sensing, or biophysics related applications.

Sun *et al.*[204] demonstrated a bio-inspired optofluidic dye laser excited by fluorescent resonance energy transfer (FRET).[205] FRET describes the mechanism of energy transfer between donor and acceptor chromophores. In this work, DNA strands were used as nano-scale scaffolds to adjust the separation between donor and acceptor chromophores. The characteristics of the FRET lasers such as spectrum, threshold, and energy conversion efficiency were reported. They claimed that through the DNA scaffolds, nearly 100% energy transfer could be maintained regardless of the donor and acceptor concentration.

Gather and Yun[203] demonstrated a dye laser, which used colonies of *E. coli* bacteria as the lasing medium. The bacteria were genetically transformed to synthesize fluorescent protein. The optical gain effect in the laser was demonstrated by clear threshold behavior and discrete peaks in the laser emission spectrum. Demonstration of lasing from bacteria and other organic biospecies proves to be an important step towards realizing self-sustainable biological lasers.

IV. SUMMARY AND FUTURE PERSPECTIVES

In this review, we described the versatile capabilities of manipulation forces in controlling, trapping, separating, sorting, and distinguishing particles in microfluidics, categorized into mechanical, electrical, thermal, optical, and magnetic forces (summarized in Table I). These forces can be applied for controlling the motion and locations of these particles either individually or in groups.

We then described novel optofluidic applications resulting from the integration of particles and optofluidics. Optical components such as tuneable waveguides and lenses and a range of particle detection platforms based on light scattering and fluorescence analysis were presented. We described several relevant implementations of manipulating SERS-active particles for enhanced Raman spectroscopy analysis in microfluidics. Finally, optofluidic applications specifically incorporating biological particles and the relatively nascent field of thermal and energy related optofluidics were discussed.

We conclude by noting that optofluidics incorporating suspended particles is a field, full of promise but is still in its infancy. Despite the numerous platforms developed as a result of considerable research in this field, we feel that there are still many areas which can be explored that could potentially result in significant outcomes as follows:

- The evolution of microfabrication methods could realize much more advanced and accurate particle manipulation platforms: in particular, more sophisticated electrodes for creating well controlled electric, magnetic, acoustic, and thermal fields as well as elements for optical fields and different morphologies of microfluidic channels. Such elements that have greater precision could be used for improved access to particles at the individual level, yielding interesting optical responses.
- Examination of waveguiding and scattering properties of individual or clusters of closely packed particles over a wide wavelength range and utilizing different particle candidates with distinct optical confinement, surface chemistry, and refractive index properties could yield promising results for developing advanced optofluidic systems.

- Introducing biological particles for investigating and expanding existing platforms' biosensing capabilities, conducting rapid and complicated assays, and developing single particle sensors controlled by actively applied forces.
- Analysis of SERS-active particles under microfluidic flow. Exploring the impact of coupling optical signals into closely packed particles and the presence of optical fields in particle dense media could result in the amplification of SERS signals producing highly sensitive Raman sensing platforms.
- Investigation of plasmonic nanostructures and particles exhibiting SPR activity and the confinement of optical waves within organic or inorganic particles would realize highly sensitive and dynamically controlled plasmonic optofluidic platforms, which are tuneable and reconfigurable.
- The creation of optofluidic systems for achieving efficient solar-based and fuel energy harvesting using photo-catalytic particles. In particular, microfluidic structures integrated with such particles permitting very high solar energy absorption could be developed.

Collectively, we anticipate that the aforementioned points form key features of forthcoming optofluidic systems, which incorporate well controlled suspended particles.

[1]C. Monat, P. Domachuk, C. Grillet, M. Collins, B. Eggleton, M. Cronin-Golomb, S. Mutzenich, T. Mahmud, G. Rosengarten, and A. Mitchell, Microfluid. Nanofluid. **4**, 1 (2008).
[2]J. M. Lim, S. H. Kim, J. H. Choi, and S. M. Yang, Lab Chip **8**, 9 (2008).
[3]P. Fei, Z. He, C. Zheng, T. Chen, Y. Men and Y. Huang, Lab Chip **11**, 17 (2011).
[4]S. Z. Malynych, A. Tokarev, S. Hudson, G. Chumanov, J. Ballato, and K. G. Kornev, J. Magn. Magn. Mater. **322**, 1894–1897 (2010).
[5]A. H. J. Yang and D. Erickson, Lab Chip **10**, 6 (2010).
[6]P. Measor, B. S. Phillips, A. Chen, A. R. Hawkins, and H. Schmidt, Lab Chip **11**, 5 (2011).
[7]D. Psaltis, S. R. Quake, and C. Yang, Nature **442**, 7101 (2006).
[8]Y. Fainman, *Optofluidics: Fundamentals, Devices, and Applications* (McGraw-Hill, New York, 2010).
[9]A. A. Kayani, A. F. Chrimes, K. Khoshmanesh, V. Sivan, E. Zeller, K. Kalantar-zadeh, and A. Mitchell, Microfluid. Nanofluid. **11**, 1 (2011).
[10]S. K. Lee, S. H. Kim, J. H. Kang, S. G. Park, W. J. Jung, S. H. Kim, G. R. Yi, and S. M. Yang, Microfluid. Nanofluid. **4**, 1–2 (2008).
[11]H. Tsutsui and C.-M. Ho, Mech. Res. Commun. **36**, 1 (2009).
[12]A. Lenshof and T. Laurell, Chem. Soc. Rev. **39**, 3 (2010).
[13]U. Levy and R. Shamai, Microfluid. Nanofluid. **4**, 1–2 (2008).
[14]H. C. Hamaker, Physica **4**, 1058–1072 (1937).
[15]S. C. Glotzer, M. J. Solomon, and N. A. Kotov, AIChE J. **50**, 12 (2004).
[16]K. Larson-Smith and D. C. Pozzo, Soft Matter **7**, 11 (2011).
[17]W. B. Russel, Annu. Rev. Fluid Mech. **13**, 425–455 (1981).
[18]D. A. Walker, C. E. Wilmer, B. Kowalczyk, K. J. M. Bishop, and B. A. Grzybowski, Nano Lett. **10**, 6 (2010).
[19]A. Böker, J. He, T. Emrick, and T. P. Russell, Soft Matter **3**, 10 (2007).
[20]K. J. M. Bishop, C. E. Wilmer, S. Soh, and B. A. Grzybowski, Small **5**, 14 (2009).
[21]Y. Liang, N. Hilal, P. Langston, and V. Starov, Adv. Colloid Interface Sci. **134–35**, 151–166 (2007).
[22]D. Di Carlo, Lab Chip **9**, 21 (2009).
[23]M. J. Rhodes, *Introduction to Particle Technology*, 2nd ed. (Wiley, Hoboken, 2008).
[24]A. Guha, *Annual Review of Fluid Mechanics* (Annual Reviews, Palo Alto, 2008), Vol. 40, pp. 311–341.
[25]G. M. Whitesides, Nature **442**, 7101 (2006).
[26]G. K. Batchelor, *An Introduction to Fluid Dynamics* (Cambridge University Press, Cambridge, 1999).
[27]J. Friend and L. Y. Yeo, Rev. Mod. Phys. **83**, 2 (2011).
[28]C. Zhang, K. Khoshmanesh, A. Mitchell, and K. Kalantar-zadeh, Anal. Bioanal. Chem. **396**, 1 (2010).
[29]R. Pethig, Biomicrofluidics **4**, 2 (2010).
[30]K. Khoshmanesh, S. Nahavandi, S. Baratchi, A. Mitchell, and K. Kalantar-zadeh, Biosens. Bioelectron. **26**, 5 (2011).
[31]K. Kleparnik and P. Bocek, Bioessays **32**, 3 (2010).
[32]B. Gas, Electrophoresis **30**, S7–S15 (2009).
[33]D. Erickson, X. Serey, Y. F. Chen, and S. Mandal, Lab Chip **11**, 6 (2011).
[34]A. Jonas and P. Zemanek, Electrophoresis **29**, 24 (2008).
[35]A. Parola and R. Piazza, Eur. Phys. J. E **15**, 3 (2004).
[36]R. Piazza and A. Parola, J. Phys. Condens. Matter **20**, 15 (2008).
[37]D. Vigolo, R. Rusconi, H. A. Stone, and R. Piazza, Soft Matter **6**, 15 (2010).
[38]M. Suwa and H. Watarai, Anal. Chim. Acta **690**, 2 (2011).
[39]S. A. Peyman, E. Y. Iwan, O. Margarson, A. Iles, and N. Pamme, J. Chromatogr. A **1216**, 52 (2009).
[40]C. Gosse and V. Croquette, Biophys. J. **82**, 6 (2002).
[41]K. Khoshmanesh, C. Zhang, F. J. Tovar-Lopez, S. Nahavandi, S. Baratchi, K. Kalantar-zadeh, and A. Mitchell, Electrophoresis **30**, 21 (2009).
[42]X. Xuan, J. Zhu, and C. Church, Microfluid. Nanofluid. **9**, 1 (2010).
[43]S. Yang, J. Y. Kim, S. J. Lee, S. S. Lee, and J. M. Kim, Lab Chip **11**, 2 (2011).
[44]S. C. Hur, H. T. K. Tse, and D. Di Carlo, Lab Chip **10**, 3 (2010).
[45]T. M. Squires and S. R. Quake, Rev. Mod. Phys. **77**, 3 (2005).

[46]J. P. Brody and P. Yager, Sens. Actuators, A **58**, 1 (1997).
[47]J. P. Brody, P. Yager, R. E. Goldstein, and R. H. Austin, Biophys. J. **71**, 6 (1996).
[48]M. Tanyeri, M. Ranka, N. Sittipolkul, and C. M. Schroeder, Lab Chip **11**, 10 (2011).
[49]M. Tanyeri, E. M. Johnson-Chavarria, and C. M. Schroeder, Appl. Phys. Lett. **96**, 22 (2010).
[50]F. Petersson, L. Aberg, A.-M. Sward-Nilsson, and T. Laurell, Anal. Chem. **79**, 14 (2007).
[51]T. Laurell, F. Petersson, and A. Nilsson, Chem. Soc. Rev. **36**, 3 (2007).
[52]D. A. Johnson and D. L. Feke, Sep. Technol. **5**, 4 (1995).
[53]T. Lilliehorn, U. Simu, M. Nilsson, M. Almqvist, T. Stepinski, T. Laurell, J. Nilsson, and S. Johansson, Ultrasonics **43**, 5 (2005).
[54]J. Shi, H. Huang, Z. Stratton, Y. Huang, and T. J. Huang, Lab Chip **9**, 23 (2009).
[55]M. Koklu, A. C. Sabuncu, and A. Beskok, J. Colloid Interface Sci. **351**, 2 (2010).
[56]H. Li, J. R. Friend, and L. Y. Yeo, Biomed. Microdevices **9**, 5 (2007).
[57]M. Evander, A. Lenshof, T. Laurell, and J. Nilsson, Anal. Chem. **80**, 13 (2008).
[58]Z. Deyl, *Electrophoresis, A Survey of Techniques and Applications* (Elsevier, New York, 1979).
[59]M. Melvin, *Electrophoresis* (John Wiley & Sons, Chichester, 1987).
[60]J. P. Landers, *Handbook of Capillary and Microchip Electrophoresis and Associated Microtechniques* (CRC, Boca Raton, 2008).
[61]H. Pohl, *Dielectrophoresis, The Behavior of Neutral Matter in Nonuniform Electric Fields*, 1st ed. (Cambridge University Press, New York, 1978).
[62]E. Morganti, C. Collini, R. Cunaccia, A. Gianfelice, L. Odorizzi, A. Adami, L. Lorenzelli, E. Jacchetti, A. Podesta, C. Lenardi, and P. Milani, Microfluid. Nanofluid. **10**, 6 (2011).
[63]E. Choi, B. Kim, and J. Park, J. Micromech. Microeng. **19**, 12 (2009).
[64]M. D. Vahey and J. Voldman, Anal. Chem. **80**, 9 (2008).
[65]B. Cetin and D. Li, Electrophoresis **32**, 18 (2011).
[66]A. Kuzyk, Electrophoresis **32**, 17 (2011).
[67]R. Piazza, Soft Matter **4**, 9 (2008).
[68]S. Duhr and D. Braun, Phys. Rev. Lett. **96**, 16 (2006).
[69]A. V. Plyukhin, Phys. Lett. A **373**, 25 (2009).
[70]S. Duhr and D. Braun, Appl. Phys. Lett. **86**, 13 (2005).
[71]J. Buongiorno, ASME Trans. J. Heat Transfer **128**, 3 (2006).
[72]M. Jerabek-Willemsen, C. J. Wienken, D. Braun, P. Baaske, and S. Duhr, Assay Drug Dev. Technol. **9**, 4 (2011).
[73]A. Ashkin, Proc. Natl. Acad. Sci. U. S. A. **94**, 10 (1997).
[74]D. G. Grier, Nature **424**, 6950 (2003).
[75]A. Ashkin, IEEE J. Sel. Top. Quantum Electron. **6**, 6 (2000).
[76]K. C. Toussaint, Jr., M. Liu, M. Pelton, J. Pesic, M. J. Guffey, P. Guyot-Sionnest, and N. F. Scherer, Opt. Express **15**, 19 (2007).
[77]A. S. Zelenina, R. Quidant, and M. Nieto-Vesperinas, Opt. Lett. **32**, 9 (2007).
[78]J. Huisken and E. H. K. Stelzer, Opt. Lett. **27**, 14 (2002).
[79]A. van der Horst, A. I. Campbell, L. K. van Vugt, D. A. M. Vanmaekelbergh, M. Dogterom, and A. van Blaaderen, Opt. Express **15**, 18 (2007).
[80]K. Dholakia, P. Reece, and M. Gu, Chem. Soc. Rev. **37**, 1 (2008).
[81]B. I. Bluestein, I. M. Walczak, and S. Y. Chen, Trends Biotechnol. **8**, 6 (1990).
[82]R. Quidant and C. Girard, Laser Photonics Rev. **2**, 1–2 (2008).
[83]S. Maier, *Plasmonics: Fundamentals and Applications* (Springer, New York, 2007).
[84]N. J. Halas, S. Lal, W.-S. Chang, S. Link, and P. Nordlander, Chem. Rev. **111**, 6 (2011).
[85]W. A. Murray and W. L. Barnes, Adv. Mater. **19**, 22 (2007).
[86]M. Righini, A. S. Zelenina, C. Girard, and R. Quidant, Nat. Phys. **3**, 7 (2007).
[87]C. Huang, J. Jiang, C. Muangphat, X. Sun, and Y. Hao, Nanoscale Res. Lett. **6**, 1–5 (2011).
[88]W. Zhang, L. Huang, C. Santschi, and O. J. F. Martin, Nano Lett. **10**, 3 (2010).
[89]M. Pelton, J. Aizpurua, and G. Bryant, Laser Photonics Rev. **2**, 3 (2008).
[90]C. Bohren and D. Huffman, *Absorption and Scattering of Light by Small Particles* (Wiley, New York, 1983).
[91]Y. G. Sun and Y. N. Xia, Anal. Chem. **74**, 20 (2002).
[92]P. Van Dorpe and J. Ye, ACS Nano **5**, 9 (2011).
[93]A. N. Grigorenko, N. W. Roberts, M. R. Dickinson, and Y. Zhang, Nat. Photonics **2**, 6 (2008).
[94]A. H. J. Yang, S. D. Moore, B. S. Schmidt, M. Klug, M. Lipson, and D. Erickson, Nature **457**, 7225 (2009).
[95]A. T. Ohta, P.-Y. Chiou, H. L. Phan, S. W. Sherwood, J. M. Yang, A. N. K. Lau, H.-Y. Hsu, A. Jamshidi, and M. C. Wu, IEEE J. Sel. Topics Quantum Electron. **13**, 2 (2007).
[96]A. Nitkowski, A. Gondarenko, and M. Lipson, Opt. Lett. **35**, 10 (2010).
[97]Y. Zhao, B. S. Fujimoto, G. D. M. Jeffries, P. G. Schiro, and D. T. Chiu, Opt. Express **15**, 10 (2007).
[98]P. Y. Chiou, A. T. Ohta, and M. C. Wu, Nature **436**, 7049 (2005).
[99]B. Kirby, *Micro- and Nanoscale Fluid Mechanics* (Cambridge University Press, Cambridge, 2010).
[100]A. Ivon Rodriguez-Villarreal, M. D. Tarn, L. A. Madden, J. B. Lutz, J. Greenman, J. Samitier, and N. Pamme, Lab Chip **11**, 7 (2011).
[101]N. Spaldin, *Magnetic Materials: Fundamentals and Applications*, 2nd ed. (Cambridge University Press, Cambridge, 2011).
[102]X. Wu, H. Wu, and Y. Hu, Microfluid. Nanofluid. **11**, 1 (2011).
[103]J. D. Adams, U. Kim, and H. T. Soh, Proc. Natl. Acad. Sci. U. S. A. **105**, 47 (2008).
[104]N. Pamme and C. Wilhelm, Lab Chip **6**, 8 (2006).
[105]J. Lim, C. Lanni, E. R. Evarts, F. Lanni, R. D. Tilton, and S. A. Majetich, ACS Nano **5**, 1 (2011).
[106]J. Kim, H.-H. Lee, U. Steinfeld, and H. Seidel, IEEE Sens. J. **9**, 8 (2009).
[107]C. Liu, T. Stakenborg, S. Peeters, and L. Lagae, J. Appl. Phys. **105**, 10 (2009).
[108]J. H. Kang and J.-K. Park, Small **3**, 10 (2007).

[109]A. J. Chung and D. Erickson, Opt. Express **19**, 9 (2011).
[110]P. Fei, Z. He, C. Zheng, T. Chen, Y. Men, and Y. Huang, Lab Chip **11**, 17 (2011).
[111]A. R. Hawkins and H. Schmidt, Microfluid. Nanofluid. **4**, 1–2 (2008).
[112]X.-T. Su, K. Singh, C. Capjack, J. Petracek, C. Backhouse, and W. Rozmus, J. Biomed. Opt. **13**, 2 (2008).
[113]R. S. Conroy, B. T. Mayers, D. V. Vezenov, D. B. Wolfe, M. G. Prentiss, and G. M. Whitesides, Appl. Opt. **44**, 36 (2005).
[114]A. Kayani, C. Zhang, K. Khoshmanesh, J. L. Campbell, A. Mitchell, and K. Kalantar-zadeh, Electrophoresis **31**, 6 (2010).
[115]K. Kalantar-zadeh, K. Khoshmanesh, A. A. Kayani, S. Nahavandi, and A. Mitchell, Appl. Phys. Lett. **96**, 10 (2010).
[116]C. Song, N.-T. Nguyen, Y. F. Yap, T.-D. Luong, and A. K. Asundi, Microfluid. Nanofluid. **10**, 3 (2011).
[117]J. P. Brody and S. R. Quake, Appl. Phys. Lett. **74**, 1 (1999).
[118]L. E. Helseth and T. M. Fischer, Opt. Express **12**, 15 (2004).
[119]J. Kneipp, X. Li, M. Sherwood, U. Panne, H. Kneipp, M. I. Stockman, and K. Kneipp, Anal. Chem. **80**, 11 (2008).
[120]M. H. Wu and G. M. Whitesides, Appl. Phys. Lett. **78**, 16 (2001).
[121]Y. Ebenstein and L. A. Bentolila, Nat. Nanotechnol. **5**, 2 (2010).
[122]J. J. Schwartz, S. Stavrakis, and S. R. Quake, Nat. Nanotechnol. **5**, 2 (2010).
[123]M. A. Bucaro, P. R. Kolodner, J. A. Taylor, A. Sidorenko, J. Aizenberg, and T. N. Krupenkin, Langmuir **25**, 6 (2009).
[124]A. Groisman, S. Zamek, K. Campbell, L. Pang, U. Levy, and Y. Fainman, Opt. Express **16**, 18 (2008).
[125]N. T. Nguyen, T. F. Kong, J. H. Goh, and C. L. N. Low, J. Micromech. Microeng. **17**, 11 (2007).
[126]Y. C. Seow, S. P. Lim, and H. P. Lee, Appl. Phys. Lett. **95**, 11 (2009).
[127]S. Zamek, B. Slutsky, L. Pang, U. Levy, and Y. Fainman, *Optofluidic Switches and Sensors* (CRC, Boca Raton, 2010).
[128]P. Domachuk, M. Cronin-Golomb, B. J. Eggleton, S. Mutzenich, G. Rosengarten, and A. Mitchell, Opt. Express **13**, 19 (2005).
[129]L. E. Helseth, H. Z. Wen, and T. M. Fischer, Langmuir **22**, 8 (2006).
[130]A. Tokarev, B. Rubin, M. Bedford, and K. G. Kornev, in *8th International Conference on the Scientific and Clinical Applications of Magnetic Carriers*, edited by U. Hafeli, W. Schutt, and M. Zborowski (American Institute of Physics, Melville, 2010), Vol. 1311, pp. 204–209.
[131]A. Candiani, W. Margulis, C. Sterner, M. Konstantaki, P. Childs, S. Pissadakis, in *Optical Sensors 2011 and Photonic Crystal Fibers V*, edited by F. Baldini, J. Homola, R. A. Lieberman, and K. Kalli (SPIE International Society of Optical Engineering, Bellingham, 2011), Vol. 8073.
[132]S. Mandal and D. Erickson, Appl. Phys. Lett. **90**, 18 (2007).
[133]H. Guo, P. Zhao, G. Xiao, Z. Zhang, and J. Yao, IEEE J. Sel. Top. Quantum Electron. **16**, 4 (2010).
[134]K. Grujic, O. G. Helleso, J. P. Hole, and J. S. Wilkinson, Opt. Express **13**, 1 (2005).
[135]V. R. Almeida, Q. F. Xu, C. A. Barrios, and M. Lipson, Opt. Lett. **29**, 11 (2004).
[136]B. Saleh and M. C. Teich, *Fundamentals of Photonics* (Wiley, Hoboken, NJ, 2007).
[137]A. H. J. Yang, T. Lerdsuchatawanich, and D. Erickson, Nano Lett. **9**, 3 (2009).
[138]X. Fan and I. M. White, Nat. Photonics **5**, 10 (2011).
[139]A. B. Matsko and V. S. Ilchenko, IEEE J. Sel. Top. Quantum Electron. **12**, 1 (2006).
[140]Y. Fainman, L. P. Lee, D. Psaltis, and C. Yang, *Optofluidics, Fundamentals, Devices and Applications* (McGraw-Hill, New York, 2010).
[141]Y. Sun and X. Fan, Anal. Bioanal. Chem. **399**, 1 (2011).
[142]H. Zhu, I. M. White, J. D. Suter, P. S. Dale, and X. Fan, Opt. Express **15**, 15 (2007).
[143]H. Cai and A. W. Poon, Opt. Lett. **35**, 17 (2010).
[144]H. Cai and A. W. Poon, Opt. Lett. **36**, 21 (2011).
[145]H. Hwang, Y.-J. Choi, W. Choi, S.-H. Kim, J. Jang, and J.-K. Park, Electrophoresis **29**, 6 (2008).
[146]W. Choi, S.-H. Kim, J. Jang, and J.-K. Park, Microfluid. Nanofluid. **3**, 2 (2007).
[147]M. Padgett and R. Di Leonardo, Lab Chip **11**, 7 (2011).
[148]C. Alpmann, M. Esseling, P. Rose, and C. Denz, Appl. Phys. Lett. **100**, 11 (2012).
[149]P. C. Ashok and K. Dholakia, Curr. Opin. Biotechnol. **23**, 1 (2012).
[150]A. E. Ekpenyong, C. L. Posey, J. L. Chaput, A. K. Burkart, M. M. Marquardt, T. J. Smith, and M. G. Nichols, Appl. Opt. **48**, 32 (2009).
[151]J. Guck, R. Ananthakrishnan, H. Mahmood, T. J. Moon, C. C. Cunningham, and J. Kas, Biophys. J. **81**, 2 (2001).
[152]A. N. Shvalov, I. V. Surovtsev, A. V. Chernyshev, J. T. Soini, and V. P. Maltsev, Cytometry **37**, 3 (1999).
[153]T. D. Perroud, J. N. Kaiser, J. C. Sy, T. W. Lane, C. S. Branda, A. K. Singh, and K. D. Patel, Anal. Chem. **80**, 16 (2008).
[154]A. Mitra, B. Deutsch, F. Ignatovich, C. Dykes, and L. Novotny, ACS Nano **4**, 3 (2010).
[155]H. Schmidt and A. R. Hawkins, Laser Photon. Rev. **4**, 6 (2010).
[156]R. Bernini, S. Campopiano, L. Zeni, and P. M. Sarro, Sens. Actuators B **100**, 1–2 (2004).
[157]S. Kuehn, E. J. Lunt, B. S. Phillips, A. R. Hawkins, and H. Schmidt, Opt. Lett. **34**, 15 (2009).
[158]S. Kuehn, B. S. Phillips, E. J. Lunt, A. R. Hawkins, and H. Schmidt, Lab Chip **10**, 2 (2010).
[159]S. Kuhn, P. Measor, E. J. Lunt, B. S. Phillips, D. W. Deamer, A. R. Hawkins, and H. Schmidt, Lab Chip **9**, 15 (2009).
[160]P. Measor, S. Kuehn, E. J. Lunt, B. S. Phillips, A. R. Hawkins, and H. Schmidt, Opt. Express **17**, 26 (2009).
[161]S. H. Cho, J. M. Godin, C.-H. Chen, W. Qiao, H. Lee, and Y.-H. Lo, Biomicrofluidics **4**, 4 (2010).
[162]H. B. Steen, Cytometry **11**, 2 (1990).
[163]J. S. Kim and F. S. Ligler, Anal. Bioanal. Chem. **398**, 6 (2010).
[164]M. Rosenauer and M. J. Vellekoop, Biomicrofluidics **4**, 4 (2010).
[165]H. Zhu, S. Mavandadi, A. F. Coskun, O. Yaglidere, and A. Ozcan, Anal. Chem. **83**, 17 (2011).
[166]Z. Wang, O. Hansen, P. K. Petersen, A. Rogeberg, J. P. Kutter, D. D. Bang, and A. Wolff, Electrophoresis **27**, 24 (2006).
[167]C. Lim, J. Hong, B. G. Chung, A. J. DeMello, and J. Choo, Analyst **135**, 5 (2010).
[168]D. J. Gardiner, P. R. Graves, H. J. Bowley, D. L. Gerrard, J. D. Louden, and G. Turrell, *Practical Raman Spectroscopy* (Springer-Verlag, New York, 1989).

[169]Y. S. Huh, A. J. Chung, and D. Erickson, Microfluid. Nanofluid. **6**, 3 (2009).
[170]M. Wang, N. Jing, I. H. Chou, G. L. Cote, and J. Kameoka, Lab Chip **7**, 5 (2007).
[171]A. F. Chrimes, A. A. Kayani, K. Khoshmanesh, P. R. Stoddart, P. Mulvaney, A. Mitchell, and K. Kalantar-zadeh, Lab Chip **11**, 5 (2011).
[172]A. F. Chrimes, K. Khoshmanesh, P. R. Stoddart, A. A. Kayani, A. Mitchell, H. Daima, V. Bansal, and K. Kalantar-zadeh, Anal. Chem. **84**, 9 (2012).
[173]I. M. White, J. Gohring, and X. Fan, Opt. Express **15**, 25 (2007).
[174]L. Tong, M. Righini, M. Ujue Gonzalez, R. Quidant, and M. Kall, Lab Chip **9**, 2 (2009).
[175]A. Y. Lau, L. P. Lee, and J. W. Chan, Lab Chip **8**, 7 (2008).
[176]P. Measor, L. Seballos, D. Yin, J. Z. Zhang, E. J. Lunt, A. R. Hawkins, and H. Schmidt, Appl. Phys. Lett. **90**, 211107 (2007).
[177]L. Huang, S. J. Maerkl, and O. J. F. Martin, Opt. Express **17**, 8 (2009).
[178]M. L. Juan, M. Righini, and R. Quidant, Nat. Photonics **5**, 6 (2011).
[179]H. M. K. Wong, M. Righini, J. C. Gates, P. G. R. Smith, V. Pruneri, and R. Quidant, Appl. Phys. Lett. **99**, 6 (2011).
[180]G. Volpe, R. Quidant, G. Badenes, and D. Petrov, Phys. Rev. Lett. **96**, 23 (2006).
[181]Y. Cheng, M. Wang, G. Borghs, and H. Chen, Langmuir **27**, 12 (2011).
[182]K. Kneipp, M. Moskovits, and H. Kneipp, *Surface-Enhanced Raman Scattering: Physics and Applications* (Springer-Verlag, Berlin, 2006).
[183]K. Wang, E. Schonbrun, P. Steinvurzel, and K. B. Crozier, Nano Lett. **10**, 9 (2010).
[184]J. Homola, S. S. Yee, and G. Gauglitz, Sens. Actuators B **54**, 1–2 (1999).
[185]W. M. Mullett, E. P. C. Lai, and J. M. Yeung, Meth. A Companion Meth. Enzymol. **22**, 1 (2000).
[186]J. Zhao, X. Y. Zhang, C. R. Yonzon, A. J. Haes, and R. P. Van Duyne, Nanomedicine **1**, 2 (2006).
[187]J. Homola, Chem. Rev. **108**, 2 (2008).
[188]W.-T. Hsu, W.-H. Hsieh, S.-F. Cheng, C.-P. Jen, C.-C. Wu, C.-H. Li, C.-Y. Lee, W.-Y. Li, L.-K. Chau, C.-Y. Chiang, and S.-R. Lyu, Anal. Chim. Acta **697**, 1–2 (2011).
[189]F. M. Weinert, C. B. Mast, and D. Braun, Phys. Chem. Chem. Phys. **13**, 21 (2011).
[190]L. H. Thamdrup, N. B. Larsen, and A. Kristensen, Nano Lett. **10**, 3 (2010).
[191]J. S. Donner, G. Baffou, D. McCloskey, and R. Quidant, ACS Nano **5**, 7 (2011).
[192]L. E. Strong and J. L. West, Wiley Interdiscip. Rev. Nanomed. Nanobiotechnol. **3**, 3 (2011).
[193]S. Duhr and D. Braun, Phys. Rev. Lett. **97**, 3 (2006).
[194]S. J. Williams, A. Kumar, N. G. Green, and S. T. Wereley, Nanoscale **1**, 1 (2009).
[195]P. Baaske, C. J. Wienken, P. Reineck, S. Duhr, and D. Braun, Angew. Chem., Int. Ed. **49**, 12 (2010).
[196]D. Erickson, D. Sinton, and D. Psaltis, Nat. Photonics **5**, 10 (2011).
[197]K. Y. Lien, L. Y. Hung, T. B. Huang, Y. C. Tsai, H. Y. Lei, and G. B. Lee, Biosens. Bioelectron. **26**, 9 (2011).
[198]Y. Jung, Y. Choi, K.-H. Han, and A. B. Frazier, Biomed. Microdevices **12**, 4 (2010).
[199]A. Lenshof, A. Ahmad-Tajudin, K. Jaras, A.-M. Sward-Nilsson, L. Aberg, G. Marko-Varga, J. Malm, H. Lilja, and T. Laurell, Anal. Chem. **81**, 15 (2009).
[200]H. Hwang, D.-H. Lee, W. Choi, and J.-K. Park, Biomicrofluidics **3**, 1 (2009).
[201]M. Kim, D. J. Hwang, H. Jeon, K. Hiromatsu, and C. P. Grigoropoulos, Lab Chip **9**, 2 (2009).
[202]M. Righini, P. Ghenuche, S. Cherukulappurath, V. Myroshnychenko, F. J. Garcia de Abajo, and R. Quidant, Nano Lett. **9**, 10 (2009).
[203]M. C. Gather and S. H. Yun, Opt. Lett. **36**, 16 (2011).
[204]Y. Sun, S. I. Shopova, C.-S. Wu, S. Arnold, and X. Fan, Proc. Natl. Acad. Sci. U. S. A. **107**, 37 (2010).
[205]E. Alvarez-Curto, J. D. Pediani, and G. Milligan, Anal. Bioanal. Chem. **398**, 1 (2010).